Macromolecules

pubs.acs.org/Macromolecules

Article

Dithiolane-Crosslinked Poly(ε-caprolactone)-Based Micelles: Impact of Monomer Sequence, Nature of Monomer, and Reducing Agent on the Dynamic Crosslinking Properties

Yanna Liu, Mies J. van Steenbergen, Zhiyuan Zhong, Sabrina Oliveira, Wim E. Hennink, and Cornelus F. van Nostrum*

Cite This: *Macromolecules* 2020, 53, 7009−7024

Read Online

ACCESS | Metrics & More | Article Recommendations | Supporting Information

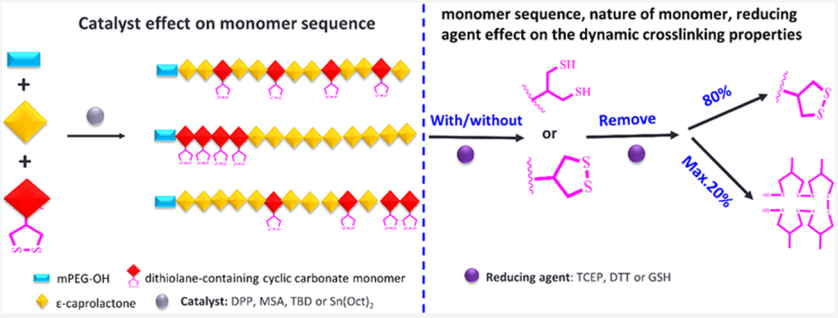

ABSTRACT: Dithiolanes are used to obtain dynamic and reversible crosslinks between polymer chains. Copolymers of two different dithiolane-containing cyclic carbonate monomers and ε-caprolactone (CL) were synthesized by ring-opening polymerization using a methoxy-poly(ethylene glycol) (mPEG) initiator and different catalysts (diphenyl phosphate (DPP), methanesulfonic acid (MSA), 1,5,7-triazabicyclo[4.4.0]dec-5-ene (TBD), or $Sn(Oct)_2$). Each catalyst required a different temperature, which had a pronounced influence on the reactivity ratio of the monomers and occurrence of transesterification reactions and, therefore, the monomer sequence. Self-crosslinkable copolymers were obtained when the dithiolane units were connected closely to the polymer backbone, whereas the presence of a linker unit between the dithiolane and the backbone prevented self-crosslinking. The former amphiphilic PEGylated block copolymers formed micelles by nanoprecipitation in the aqueous environment and crosslinked spontaneously by disulfide exchange during subsequent dialysis. These dithiolane-crosslinked micelles showed reduction-responsive dissociation in the presence of 10 mM glutathione, making them promising drug delivery systems for the intracellularly triggered cargo release.

1. INTRODUCTION

Ring-opening polymerization (ROP) of cyclic esters and/or carbonates has attracted interest for many years, since the resulting polymers, *i.e.*, polyesters, polycarbonates, and poly(ester-*co*-carbonate)s, are biodegradable and biocompatible and, as such, are particularly appealing for pharmaceutical and biomedical applications, *e.g.*, nanoparticulate drug carriers and tissue engineering.[1−5] ROP of cyclic esters and/or carbonates has been extensively studied using various types of catalysts, *e.g.*, basic organocatalysts like 1,5,7-triazabicyclo[4.4.0]dec-5-ene (TBD), acid organocatalysts like sulfonic acids, and metallic catalysts like $Sn(Oct)_2$. Catalysis mechanisms are greatly different, *e.g.*, bifunctional activation mechanism by TBD vs coordination−insertion by a metallic catalyst.[6−8] These different mechanisms might lead to different polymerization behaviors of monomers, thus yielding copolymers with different structural parameters, *e.g.*, composition, microstructure (*i.e.*, the monomer sequence), and polydispersity, which are important factors that determine the properties of polymers, and thus their applications.[9−13] For instance, it has been demonstrated that an acidic organocatalyst, diphenyl phosphate (DPP), and a basic organocatalyst, TBD, have different ring-opening copolymerization behaviors of cyclic carbonate-based monomers, leading to copolymers with random and blocky microstructures, respectively.[13] In this regard, understanding the role of the catalyst in the kinetics of polymerization becomes important since it offers an important opportunity to satisfy different applications by preparing polymers with different molecular features (monomer sequence, predictable molar masses, narrow molecular weight distribution, etc.) *via* catalytic tuning.

Received: April 30, 2020
Revised: July 15, 2020
Published: August 3, 2020

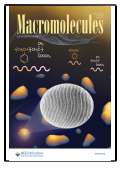

https://dx.doi.org/10.1021/acs.macromol.0c01031
Macromolecules 2020, 53, 7009−7024

Polymeric micelles prepared from biodegradable (co)-polymers have received extensive interest as delivery systems for, *e.g.*, anticancer drugs, owing to their advantageous features such as improved aqueous solubility of encapsulated hydrophobic drugs, selective accumulation at the tumor sites *via* enhanced permeability and retention (EPR) effects,[14−18] and decreased systemic side effects.[16,19,20] However, although polymeric micelles are promising nanocarriers, they are still challenged by their instability in the circulation, which often lead to premature drug release, diminished ability to selectively reach target sites, and suboptimal therapeutic efficacy.[16,21−23] To address these drawbacks, reversible crosslinking of polymeric micelles particularly using reduction-sensitive disulfide linkages is a highly attractive approach, enabling stability in the circulation and triggering drug release by de-crosslinking at the target site, *i.e.*, the cytoplasm or the cell nucleus in tumor cells.[18,24−26] This was shown in the pioneering work by Regen et al., who demonstrated the use of cyclic 1,2-dithiolanes to crosslink and thus stabilize liposomes.[27] Dithiolane-crosslinked nanoparticles based on lipoic acid were later shown to display enhanced stability under physiological conditions and triggered intracellular drug release after being de-crosslinked in the cytoplasm of cancer cells.[28] Recently, a series of tumor-targeted core-crosslinked micelles and polymersomes based on pendant dithiolanes have shown efficient delivery of doxorubicin and siRNA to tumor xenografts in nude mice.[29−36] Similar chemistry has also been used to generate dynamically crosslinked hydrogels.[37] The necessary conditions and mechanism to generate dithiolane-derived crosslinking in nanoparticles have been described in several publications. Some studies showed that crosslinking of dithiolanes in nanoparticles requires a reducing agent (RA) (*e.g.*, dithiothreitol (DTT); typically 10−50 mol % RA to disulfide bonds) that induces the disulfide exchange ring-opening polymerization of cyclic dithiolanes initiated by sulfhydryl (−SH) groups.[27,28,37−42] On the other hand, in other studies, it has been described that dithiolane-crosslinked nanoparticles are formed spontaneously when these dithiolane-containing polymers are dispersed in water (*i.e.*, without the need of free thiol as the initiator).[29−32,43] However, no existing study provides a comprehensive and detailed exploration of the dithiolane-crosslinked network in nanoparticles or potentially influential factors (*e.g.*, polymer structure, the presence of reducing agents, and concentrations).

In the present paper, we introduce pendant dithiolane rings as crosslinkable moieties in poly(ε-caprolactone)-*b*-poly(ethylene glycol) (pCL-PEG) block copolymers by ring-opening copolymerization of ε-caprolactone (CL, a cyclic ester) with a dithiolane-substituted cyclic carbonate with or without a flexible diester linker between the dithiolane ring and the cyclic carbonate unit (*i.e.*, 1,2-dithiolane-substituted trimethylene carbonate (DTC) and 1,2-dithiolane-4-diester-functionalized trimethylene carbonate (DdeTC), respectively) (Figure 1). Both monomers have been described before as crosslinkable units in polycarbonates and poly(ester carbonate)s.[29,31,32,37,42] Since, as explained above, different catalysts might yield copolymers with different monomer sequences, and thus likely different crosslinking behaviors, the influence of the selected catalyst on (co)polymerization behavior of CL and carbonate monomers was evaluated. Therefore, three different types of catalysts, *i.e.*, acidic (DPP or methanesulfonic acid (MSA)), basic (TBD), or metallic ($Sn(Oct)_2$), were used as catalysts in the ROP of CL and DTC using PEG-OH (2 kDa) as initiator, and the polymerization kinetics and the monomer sequence of the obtained block copolymers were studied by ^1H and ^{13}C NMR analyses. Subsequently, micelles based on the obtained p(CL-*co*-DTC)-PEG and p(CL-*co*-DdeTC)-PEG were prepared using a nanoprecipitation method. The rate and extent of crosslinking of these micelles in the presence and absence of different reducing agents, namely, Tris(2-carboxyethyl)-phosphine hydrochloride (TCEP), DTT, and glutathione (GSH), were investigated by *in situ* monitoring of the UV absorbance over time of the dithiolane pendant rings. Moreover, the reversibility of the crosslinking and the reductive response of the dithiolane-crosslinked p(CL-*co*-DTC)-PEG micelles in the presence of TCEP or GSH were evaluated to gain insight into the aimed behavior of the micelles in tumor cells, *i.e.*, intracellular drug release.

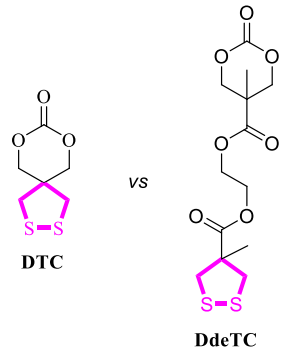

Figure 1. Structures of the 1,2-dithiolane- and 1,2-dithiolane-4-diester-substituted trimethylene carbonates (*i.e.*, DTC and DdeTC).

2. EXPERIMENTAL SECTION

2.1. Materials. 2-((4-Methyl-1,2-dithiolane-4-carbonyl)oxy)ethyl-5-methyl-2-oxo-1,3-dioxane-5-carboxylate (*i.e.*, 1,2-dithiolane-4-diester-functionalized trimethylene carbonate, DdeTC) was synthesized as previously described (Scheme S1; $^1H/^{13}C$ NMR spectra in Figures S18 and S19 in the Supporting Information).[37,42,44] 7,9-Dioxa-2,3-dithiaspiro[4.5]decan-8-one (*i.e.*, 1,2-dithiolane-substituted trimethylene carbonate, DTC) was kindly provided by Prof. Zhiyuan Zhong (Soochow University, Suzhou, China). ε-Caprolactone (CL), methoxy-poly(ethylene glycol) (mPEG-OH, 2000 g/mol), tin(II) 2-ethylhexanoate ($Sn(Oct)_2$), diphenyl phosphate (DPP, 99%), methanesulfonic acid (MSA, ≥99.0%), 1,5,7-triazabicyclo[4.4.0]dec-5-ene (TBD, 98%), Tris(2-carboxyethyl)phosphine hydrochloride (TCEP), 1,4-dithiothreitol (DTT, ≥99%,), L-glutathione (GSH, ≥98%), and triethylamine (TEA) were obtained from Sigma-Aldrich (Zwijndrecht, the Netherlands). Phosphate-buffered saline (PBS, pH 7.4, containing 11.9 mM phosphates, 137 mM sodium chloride, and 2.7 mM potassium chloride) was obtained from Fischer Bioreagents (Bleiswijk, the Netherlands). Standard regenerated cellulose dialysis tubing (Spectra/Por6) with a molecular weight cutoff (MWCO) of 1 kDa was purchased from Spectrumlabs (Rancho Dominguez, California). Ellman's reagent (5,5-dithio-bis-(2-nitrobenzoic acid)) was purchased from Fisher Scientific (Loughborough, U.K.). All other solvents and reagents were obtained from Biosolve (Valkenswaard, the Netherlands). mPEG-OH was azeotropically dried from toluene prior to use. Dichloromethane (DCM, peptide synthesis grade) and toluene were dried over 4 Å molecular sieves (Sigma-Aldrich, Zwijndrecht, the Netherlands) prior to use. All other reagents were used as received.

2.2. Synthesis of (Co)polymers. *2.2.1. Simultaneous Ring-Opening (Co)polymerization. 2.2.1.1. Copolymerization of CL and DTC Catalyzed by DPP, MSA, or TBD.* The copolymerization of CL and DTC was initiated by mPEG-OH (2000 g/mol) and catalyzed by different agents (DPP, MSA, or TBD). A representative procedure for the synthesis of p(CL-*co*-DTC)-PEG (entry 2, Table 1) catalyzed by MSA was carried out as previously described with slight modifications.[9,45] CL (410 mg, 3.6 mmol), DTC (308 mg, 1.6 mmol), and

https://dx.doi.org/10.1021/acs.macromol.0c01031
Macromolecules 2020, 53, 7009−7024

Table 1. Characteristics of Copolymers Obtained by Simultaneous and Sequential Polymerization of CL and/or DTC or DdeTC with Different Catalysts

						^{1}H NMR[a]			GPC			DSC	
entry	abbreviation of the obtained copolymers	catalyst	order of monomer addition	aimed M_n[b]	reaction time (h)	CL/DTC or DdeTC conversion (%)	M_n[b]	microstructure of copolymers	M_w[b]	M_n[b]	M_w/M_n	T_g/T_m (°C)	ΔH_m (J/g)
1	p(CL_9-$DTC_{3.8}$)-PEG	DPP	simultaneous	4.0	28	91/94	3.9	random	2.9	2.7	1.07	−36/42	81
2	p(CL_9-$DTC_{3.9}$)-PEG	MSA	simultaneous	4.0	10	100/95	4.0	random	2.9	2.7	1.07	−36/42	82
3	p($CL_{8.4}$-$DTC_{3.9}$)-PEG	TBD	simultaneous	4.0	18	76/100	3.9	random	3.5	2.9	1.21	−40/43	85
4	p($CL_{10.1}$-$DTC_{3.1}$)-PEG	$Sn(Oct)_2$	simultaneous	4.0	19	100/75	4.0	gradient	2.9	2.7	1.10	−37/42	94
5	p($CL_{9.1}$-*b*-$DTC_{4.1}$)-PEG	MSA	DTC first, then CL	4.0	18/2	100/100	4.0	blocky	2.5	2.4	1.07	−43/41	92
6	p($DTC_{3.8}$-*b*-CL_9)-PEG	MSA	CL first, then DTC	4.0	2/18	100/97	4.0	blocky	2.7	2.6	1.05	−42/40	92
7	$pCL_{9.1}$-PEG	MSA	CL only	3.2	2	100/−	3.2		2.5	2.4	1.05	−/45	125
8	$pDTC_4$-PEG	MSA	DTC only	3.0	18	−/92	3.0		2.0	2.0	1.03	−6.3/43	131
9	p(CL_9-$DTC_{3.9}$)-PEG	TBD	DTC first, then CL	4.0	0.5/12	97/100	4.0	random	4.7	3.6	1.31	−40/43	80
10	p($DTC_{4.3}$-*b*-$CL_{8.9}$)-PEG	TBD	CL first, then DTC	4.0	12/12	79/94	4.0	blocky	2.7	2.6	1.03	−36/40	92
11	$pCL_{8.8}$-PEG	TBD	CL only	3.2	12	79/−	3.2		2.4	2.3	1.04	−/49	122
12	$pDTC_{3.7}$-PEG	TBD	DTC only	3.0	0.5	−/100	3.0		3.5	2.0	1.75	−/42	130
13	p(CL_9-$DTC_{6.6}$)-PEG	MSA	simultaneous	4.8	10	97/90	4.5	random	3.0	2.9	1.07	−17/40	82
14	p(CL_{18}-$DTC_{7.5}$)-PEG	MSA	simultaneous	5.8	10	95/98	5.7	random	4.0	3.6	1.11	−31/36	61
15[c]	p(CL_9-$DdeTC_{3.1}$)-PEG	MSA	simultaneous	4.7	10	97/96	4.3	random	3.3	2.8	1.16	−40/40	95
16[c]	$pDdeTC_5$-PEG	MSA	DdeTC only	4.6	10	−/75	3.9		3.0	2.9	1.08	−17/43	67
17	mPEG-OH								1.8	1.8	1.03	−/48	182

[a]^{1}H NMR spectra of the polymers and the assignments of the corresponding NMR peaks are shown in Figures S20−S35 of the Supporting Information. [b]Units are in kDa. [c]These polymers were synthesized using DdeTC as the (co)monomer, while the other copolymers (entries 1−14) were synthesized using DTC as the co(monomer).

mPEG-OH (800 mg, 0.4 mmol) were dissolved in 6 mL dry DCM, followed by the addition of MSA (50 mg, 0.52 mmol) (CL/DTC/mPEG-OH/MSA molar ratio: 9/4/1/1.3) with agitation to initiate polymerization. The polymerization proceeded at 37 °C for 10 h under a N_2 atmosphere, and then TEA (0.52 mmol, equimolar to MSA) was added to neutralize the catalyst and terminate the reaction. The reaction solution was subsequently dropped into a 20-fold excess of cold diethyl ether (−20 °C) and the precipitate, collected by filtration, was dried under vacuum to give the final product (entry 2 in Table 1) as a slightly yellow solid (1100 mg, yield: 71%).

The copolymerization of CL and DTC using DPP or TBD as catalyst followed a similar procedure with slight modifications: molar ratios of CL/DTC/mPEG-OH/DPP and CL/DTC/mPEG-OH/TBD were adjusted to 9/4/1/10[13] and 9/4/1/0.25,[46] respectively. The applied reaction times are shown in Table 1, and when TBD was used as catalyst, the reaction was carried out at room temperature (RT) and the termination reagent was replaced by benzoic acid. The yields for the polymerizations catalyzed by DPP and TBD were 70 and 55%, respectively.

As references, pCL-PEG (entries 7 and 11, Table 1) and pDTC-PEG block copolymers (entries 8 and 12, Table 1) were synthesized using MSA or TBD as catalyst under the same conditions, by polymerization of only CL or DTC, respectively. The polymers were precipitated in cold diethyl ether (−20 °C) to obtain the pCL-PEG block copolymer as a white powder (yield: ∼60% in both cases) and the pDTC-PEG block copolymer as a yellowish solid (yield: ∼65% in both cases).

2.2.1.2. Copolymerization of CL and DTC Catalyzed by $Sn(Oct)_2$. CL (205 mg, 1.8 mmol), DTC (154 mg, 0.8 mmol), and mPEG-OH (400 mg, 0.2 mmol) were dissolved in 3 mL dry toluene. Then, a catalytic amount of $Sn(Oct)_2$ (1 mg, 0.01 mmol) (CL/DTC/mPEG-OH/$Sn(Oct)_2$ molar ratio: 9/4/1/0.05) was added, and the reaction was allowed to proceed at 110 °C for 19 h under a N_2 atmosphere. Subsequently, the cooled reaction solution was dropped into a 20-fold excess of cold diethyl ether (−20 °C). The precipitate was recovered by filtration and dried under vacuum to give the final product (entry 4 in Table 1) as a slightly yellow solid (500 mg, yield: 63%).

2.2.1.3. (Co)polymerization of CL and DdeTC Catalyzed by MSA. DdeTC without or with CL was (co)polymerized using mPEG-OH as the initiator and MSA as the catalyst (the molar ratios of DdeTC/mPEG-OH/MSA and DdeTC/CL/mPEG-OH/MSA were 8/1/1.3 and 4/9/1/1.3, respectively), following a similar procedure as described in Section 2.2.1.1, except that DTC was substituted by DdeTC. The obtained polymer was precipitated in cold diethyl ether (−20 °C). After drying under vacuum, p(CL-*co*-DdeTC)-PEG (entry 15, Table 1) was obtained as a slightly yellow solid (700 mg, yield: 55%) and pDdeTC-PEG block copolymer (entry 16, Table 1) as a yellowish solid (500 mg, yield: 45%).

2.2.2. Sequential Ring-Opening (Co)polymerization. 2.2.2.1. Polymerization with Sequential Feeding of DTC First Followed by CL. Sequential copolymerization of DTC first and then CL using MSA as the catalyst (entry 5, Table 1) was carried out as follows: to the solution of DTC (154 mg, 8 mmol) and mPEG-OH (400 mg, 0.2 mmol) in 3 mL DCM, MSA (25 mg, 0.26 mmol) was added with agitation. After stirring for 18 h at 37 °C under a N_2 atmosphere, CL (201 mg, 1.8 mmol) was introduced into the reaction mixture. The reaction continued at 37 °C under a N_2 atmosphere for 2 h and was then terminated by the addition of TEA (equal molar to MSA). The final molar ratio of CL/DTC/mPEG-OH/MSA was 9/4/1/1.3. Next, the reaction solution was dropped into a 20-fold excess of cold diethyl ether (−20 °C), and the precipitate was collected by filtration and dried under vacuum overnight to give the final product as a yellowish solid (500 mg, yield: 66%).

https://dx.doi.org/10.1021/acs.macromol.0c01031
Macromolecules 2020, 53, 7009−7024

The copolymerization with the sequential feeding of DTC first followed by CL and catalyzed by TBD was conducted at RT following a procedure similar to that mentioned above, with a slight adjustment of reaction times as shown in Table 1 (entry 9) and the molar feed ratio of CL/DTC/mPEG-OH/TBD (9/4/1/0.25). The polymer was precipitated in cold diethyl ether (−20 °C), and the yield was ∼65%.

2.2.2.2. Polymerization with Sequential Feeding of CL First Followed by DTC. Sequential copolymerization of CL followed by DTC using MSA or TBD as the catalyst was conducted following a similar procedure as mentioned in Section 2.2.2.1, but with a slight modification of the polymerization times, as shown in Table 1 (entries 6 and 10). The copolymers were precipitated in cold diethyl ether (−20 °C), and the final copolymers (entries 6 and 10, Table 1) were obtained as yellowish and slightly sticky solids (yield: ∼60% for both cases).

2.3. Polymerization Kinetics. Polymerization kinetics was determined as follows: 20 μL samples of the reaction solutions during polymer synthesis (as described in Section 2.2.1) were withdrawn at different time points using a syringe and transferred into an NMR tube containing 0.8 mL $CDCl_3$ and an excess amount of the corresponding compound that was used to terminate the reaction (see Section 2.2.1.1), and the ^{1}H NMR spectrum was subsequently recorded. The conversion of CL, DTC, or DdeTC was determined by, respectively, comparing the integrals of the peaks at 2.66 ppm (two protons of methylene from CL), 3.07 ppm (four protons of the dithiolane ring from the DTC unit), or 4.70 ppm (two protons of trimethylene carbonate (TMC) from DdeTC monomer) at each time point to its corresponding integral at the start of the experiment. The peak originating from the three methoxy protons of mPEG-OH at 3.37 ppm was used as the reference peak to normalize the integrals. The total polymerization times reported in Table 1 were established by the time that the plateau conversions were reached based on ^{1}H NMR analysis.

2.4. Polymer Characterization. ^{1}H/^{13}C NMR spectra were recorded using a Bruker NMR spectrometer (600 MHz, Bruker), with chemical shifts reported in parts per million downfield from tetramethylsilane. Polymers were dissolved in $CDCl_3$ at concentrations of approximately 15 mg/mL. Chemical shifts of the residual solvent ($CHCl_3$: δ 7.26 and 77 for proton and carbon spectra, respectively) were used as the reference lines. Peak multiplicity is denoted as s (singlet), d (doublet), dd (double doublet), t (triplet), q (quartet), m (multiplet), and b (broad signal). Based on ^{1}H NMR spectra, the average degree of polymerization (DP) of CL, DTC, or DdeTC in the obtained copolymers was determined from the ratio of the integrals of the CH_2 protons of the CL units (1.39 ppm, $CH_2CH_2\underline{\boldsymbol{CH_2}}CH_2CH_2$), the protons of the DTC units (2.97 ppm, $C\underline{\boldsymbol{CH_2}}SS\underline{\boldsymbol{CH_2}}C$), or the DdeTC units (2.92 ppm, $C\underline{\boldsymbol{CH_2}}SS\underline{\boldsymbol{CH_2}}C$) to the methyl protons of mPEG-OH (3.37 ppm, $\underline{\boldsymbol{CH_3}}O$) (eqs 1−3), respectively. The number average molecular weight (M_n) of the polymers was thus calculated from the resulting DP of CL, DTC, and DdeTC units

$$\text{DP of CL} = \frac{\text{integral (H at 1.39 ppm)}/2}{\text{integral (H at 3.37 ppm)}/3} \quad (1)$$

$$\text{DP of DTC} = \frac{\text{integral (H at 2.97 ppm)}/4}{\text{integral (H at 3.37 ppm)}/3} \quad (2)$$

$$\text{DP of DdeTC} = \frac{\text{integral (H at 2.92 ppm)}/2}{\text{integral (H at 3.37 ppm)}/3} \quad (3)$$

Gel permeation chromatography (GPC, Waters Alliance 2695 system equipped with two PLgel Mesopore columns (300 × 7.5 mm^2, including a guard column, 50 × 7.5 mm^2)) was performed using dimethylformamide (DMF) containing 10 mM LiCl as the solvent at a flow rate of 1.0 mL/min at 65 °C. A differential refractive index (RI) detector was used to record the chromatograms. Fifty microliters of 3−5 mg/mL samples dissolved in DMF containing 10 mM LiCl were injected onto the column. The number average molecular weight (M_n), weight average molecular weight (M_w), and the molecular weight distribution (M_w/M_n) of the obtained copolymers were calculated by Empower 32 software using narrow poly(ethylene glycol) standards ranging from 430 to 26 100 g/mol (from PSS, Mainz, Germany) for calibration.

Differential scanning calorimetry (DSC) was carried out using a Discovery DSC, TA Instruments, calibrated with indium. The samples (∼5 mg) were heated with a ramp of 3 °C/min up to 150 °C (modulated), annealed for 5 min, cooled down at 3 °C/min to −80 °C (modulated), again annealed for 5 min, and subsequently heated with 3 °C/min up to 150 °C (modulated). Melting temperatures (T_m) were obtained from the onset of the peaks of the total heat flow, and the melting enthalpies (ΔH_m) were recorded from the total heat flow. Glass-transition temperatures (T_g) are defined as the point of inflection of the step change observed in the reversing heat flow curve. Data of the second heating cycle were recorded.

2.5. Influence of Different Reducing Agents on the Dynamic Crosslinking of Micelles. Micellar dispersions were prepared from the obtained block copolymers by a nanoprecipitation method.[47] In short, a solution of the copolymer in DMF (40 mg/mL of p(CL-*co*-DTC)-PEG or 100 mg/mL of p(CL-*co*-DdeTC)-PEG) was added dropwise to PBS at a 1/9 volume ratio. A homogeneous micellar dispersion was formed after gentle shaking by hands. Various reducing agents (RA, *i.e.*, DTT, TCEP, or GSH, as solutions in PBS), at molar ratios of RA to the dithiolane rings present in the micellar dispersion ranging from 0 to 2, were added to the micellar dispersion, followed by adjusting to the same volume by the addition of a certain volume of PBS. After incubation with RA at 37 °C for 7 h, the different micellar dispersions were dialyzed with a dialysis tubing (MWCO = 1 kDa) against PBS at RT for 12 h.[31] The absorbance of the dithiolane rings in DTC and DdeTC units at λ = 326 and 328 nm, respectively, was recorded from the micellar samples withdrawn at different time points before and after dialysis using a Shimadzu UV-2450 spectrophotometer (Shimadzu, Japan). In addition, the samples collected from the above-mentioned micellar dispersions were freeze-dried and subsequently re-dispersed in DMF at 5 mg/mL for GPC analysis, as described in Section 2.4. Ellman's assay was performed according to the manufacturer's protocol to quantify the concentration of sulfhydryl (−SH) groups present in the micellar dispersions before and after dialysis.

2.6. De-Crosslinking of Micelles by Reducing Agents. The response of the dithiolane core-crosslinked micelles toward various reducing agents was determined by dynamic light scattering (DLS) and GPC analysis. Briefly, spontaneously crosslinked micelles were prepared by the nanoprecipitation method (without exposure to RA), *i.e.*, by the dropwise addition of the polymer solution in DMF to PBS (pH 7.4) at a volume ratio of 1:9 followed by dialysis against PBS for 12 h, as described in Section 2.5. The micelles were subsequently incubated either with 2 equiv of TCEP (a 30 mg/mL solution in PBS) relative to dithiolanes or with PBS (the same volume as the TCEP solution) for 2 h at 37 °C. Thereafter, DMF or PBS was added at a volume ratio of 1:4 at RT for 24 h. The *Z*-average hydrodynamic diameter (Z_{ave}) and polydispersity index (PDI) of the micelles before and after the addition of DMF or PBS were determined by DLS at a fixed scattering angle of 173° at 25 °C using a ZetaSizer Nano S (Malvern).

Besides, the spontaneously crosslinked micellar dispersions were incubated with TCEP, DTT, or GSH dissolved in PBS (final concentration of 10 mM) for 7 h at 37 °C. Next, the micellar dispersions were freeze-dried and then dispersed in DMF at 5 mg/mL, followed by filtration (0.22 μm) for GPC analysis, as described in Section 2.4.

2.7. Reversibility of the Crosslinking in Micelles. To investigate the reversibility of the dithiolane crosslinking, the micelles crosslinked by TCEP and subsequently dialyzed as described in Section 2.5 were aged for 96 h at RT (referred to as the first cycle). The resulting crosslinked micelles were incubated with TCEP, using molar ratios to the dithiolanes ranging from 0 to 2 for 7 h at 37 °C, dialyzed against PBS for 12 h, and after dialysis in PBS were aged for the indicated time points at RT (referred to as the second cycle). In addition, the samples collected from the micellar dispersions were freeze-dried and then dissolved in DMF at 5 mg/mL. The samples were filtered (0.22 μm) and then analyzed by GPC analysis, as described in Section 2.4.

https://dx.doi.org/10.1021/acs.macromol.0c01031
Macromolecules 2020, 53, 7009−7024

Scheme 1. Ring-Opening Polymerization of CL with Two Different Dithiolane-Based Monomers Initiated by mPEG-OH: Simultaneous Copolymerization with (A) DTC and (B) DdeTC

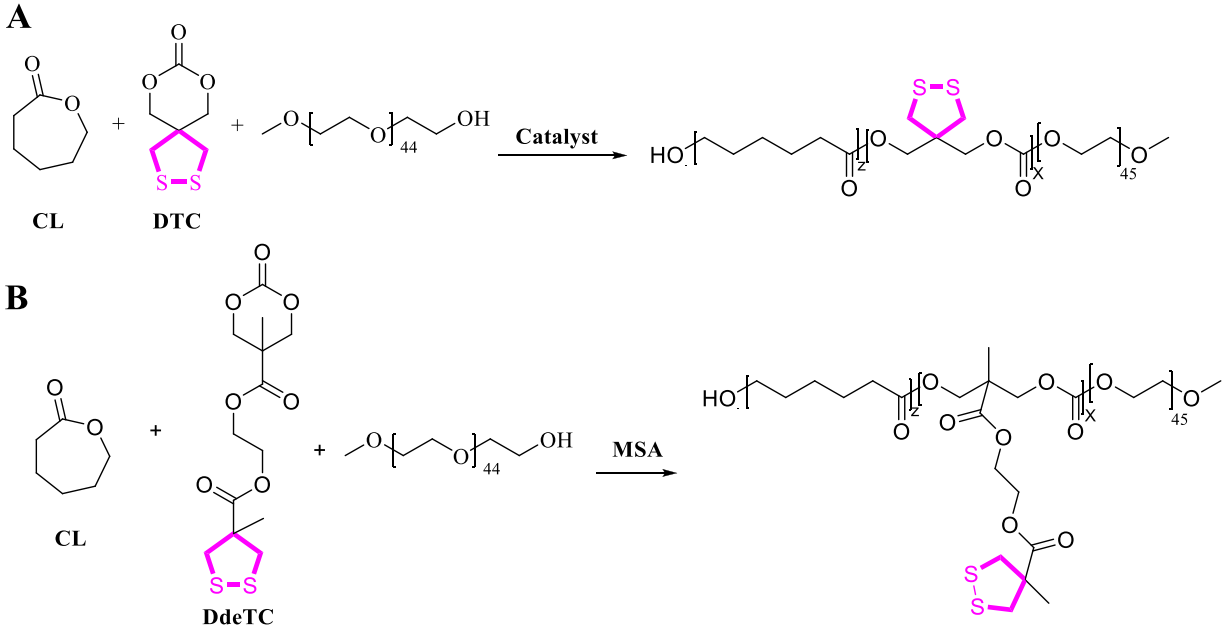

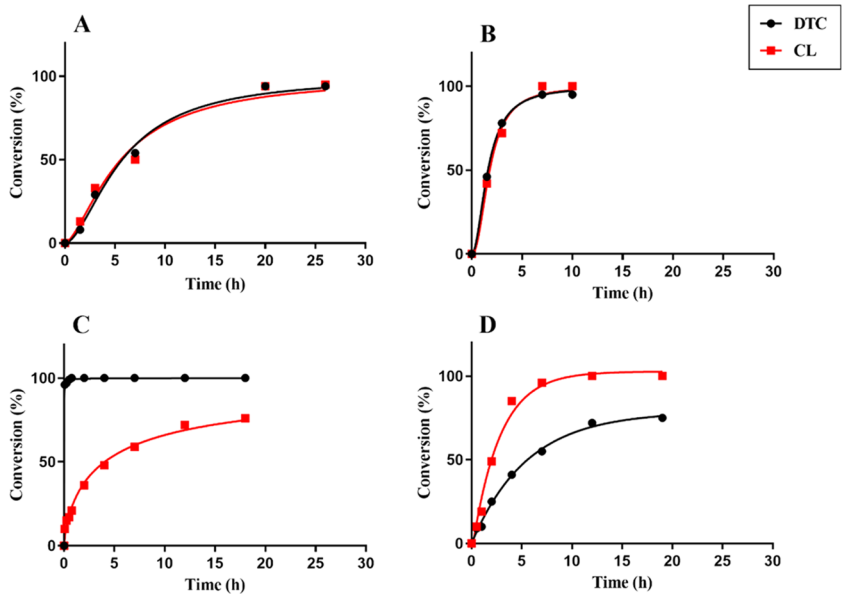

Figure 2. Conversion of CL (red squares) and DTC (black dots) monitored by ^{1}H NMR as a function of time using (A) DPP, (B) MSA, (C) TBD, and (D) Sn(Oct)$_2$ as the catalysts, with a CL/DTC/initiator molar ratio of 9/4/1 (entries 1−4, Table 1). The ROP reaction was conducted in DCM at 37 °C using DPP and MSA as the catalysts, in DCM at RT using TBD as the catalyst, and in toluene at 110 °C using Sn(Oct)$_2$ as the catalyst.

3. RESULTS AND DISCUSSION

3.1. Effect of Catalyst on the Monomer Sequence in the Copolymers. *3.1.1. Copolymers Synthesized by Simultaneous Ring-Opening Copolymerization of CL with DTC or DdeTC.* Simultaneous ROP of CL and DTC initiated by the macroinitiator mPEG-OH at a CL/DTC/PEG molar ratio of 9/4/1 (Scheme 1A) was carried out using different catalysts, *i.e.*, acidic (DPP or MSA), basic (TBD), or metallic (Sn(Oct)$_2$), to investigate the effect of the type of catalyst on the monomer sequence in the obtained copolymers (structures of these catalysts are shown in Figure S1 of the Supporting Information). To this end, the conversion of each monomer was measured by ^{1}H NMR analysis, and the relative reactivities of both monomers were determined by monitoring the decrease of peak integrals of methylene of CL at 2.66 ppm and the dithiolane ring in DTC at 3.07 ppm. 1.3 equiv of MSA relative to the initiator (Figure 2B) displayed almost complete conversion of both monomers in 7 h, while it took 28 h when using 10 equiv of DPP (Figure 2A), indicating a much higher catalytic activity for MSA. As reported in the literature, acid (DPP or MSA)-catalyzed ROP proceeds *via* a bifunctional activation mechanism; *i.e.*, these catalysts act simultaneously both as a hydrogen-bond donor to the carbonyl oxygen in the monomers and as a hydrogen-bond acceptor to the hydroxyl proton of the propagating alcohol, achieving the activation of both the electrophile and the nucleophile (Scheme S2A,B in the Supporting Information).[48,49] Therefore, the

https://dx.doi.org/10.1021/acs.macromol.0c01031
Macromolecules 2020, 53, 7009−7024

difference in reactivity of the two catalysts can be ascribed to the higher acidity of the hydrogen atom (H-bonding donor) in MSA ($pK_a = -0.6$)[50] than that in DPP ($pK_a = 2$),[48] resulting in higher electrophilic activity and shortening of the polymerization time. Importantly, Figure 2A,B shows that CL and DTC displayed similar polymerization rates for both acidic catalysts, suggesting random incorporation of both monomers in the propagating chains. The DPP-catalyzed copolymerization is in line with the findings reported by Wei et al., who showed similar polymerization rates of DTC and another carbonate-based monomer (*i.e.*, trimethylene carbonate, TMC), which indeed led to a random pDTC/poly(TMC) (pTMC) copolymer.[13] However, using MSA as the catalyst, Couffin et al. reported a higher reactivity of CL than that of TMC leading to gradient copolymers,[9] which may indicate that the reactivity of the cyclic carbonate is influenced by the substituents. It is noted that under MSA catalysis, polymerization kinetics of CL and DdeTC (Figure S2, Supporting Information) was also similar and comparable to that observed with CL and DTC (Figure 2B), suggesting that DTC and DdeTC have comparable reactivity. The comparable reactivity of cyclic ester CL and cyclic carbonates (DTC or DdeTC) under acidic catalysis is probably attributed to the electrophilic activation of both monomers, thereby minimizing possible charge density differences on the carbonyl C-atom caused by their intrinsic structures.

In contrast to the acid-catalyzed ROP, CL had a significantly lower polymerization rate than DTC when basic TBD was used as the catalyst: CL needed 18 h to achieve a 76% conversion, whereas DTC was quantitatively consumed within 30 min (Figure 2C). These large differences in reactivity lead to preferential DTC incorporation at the start of the polymerization reaction, which in turn results in a block copolymer structure of the hydrophobic polyester/carbonate segment if no transesterification and chain termination occurred. In a previous study, when DTC was copolymerized with TMC, DTC had also significantly higher reactivity than the comonomer using TBD as the catalyst, indeed yielding a blocky copolymer.[13] From a mechanistic point of view, TBD-catalyzed ROP most likely also proceeds *via* a bifunctional activation mechanism as mentioned above for acidic catalysis (Scheme S2A–C in the Supporting Information).[51] However, the obvious difference between the acidic and basic catalysts is that in the latter case, the monomers are activated by the nucleophilic attack of the amine nitrogen in TBD to the carbonyl of the monomers along with the transfer of the adjacent protonated nitrogen to the oxygen in monomers (*i.e.*, the incipient alkoxide) to generate the TBD amide (as shown in Scheme S2C of the Supporting Information). Thus, the different reactivities of DTC and CL can probably be explained by the more active intermediate TBD amide formed from cyclic carbonate (DTC) than that formed from the cyclic ester (CL), due to the presence of the extra oxygen atom as an electron-withdrawing group on the β-position that facilitates esterification with the hydrogen-bond-activated alcohol (the final step in Scheme S2C of the Supporting Information). On the contrary, in the metallic $Sn(Oct)_2$-catalyzed ROP (Figure 2D), CL reacted slightly faster than DTC (96 vs 55% conversion for CL and DTC, respectively, after 7 h), which is consistent with a previous observation on the $Sn(Oct)_2$-catalyzed random copolymerization of CL and TMC at 120 °C.[52] This suggests the possible formation of a gradient copolymer, whose monomer composition varies gradually along the growing polymer chain, assuming that no termination and transesterification occur.[10,53] The ROP catalyzed by $Sn(Oct)_2$ operates by a "coordination–insertion" mechanism, consisting of initiating an alcohol by an "*in situ*"-formed stannous alkoxide with $Sn(Oct)_2$ and propagating the polymer chain by monomer insertion into the $-S_n-O-$ bond (Scheme S2D in the Supporting Information).[54] With this coordination–insertion mechanism, the driving force for the polymerization of CL is most likely the favorable release of torsional strain in a seven-membered CL ring.[55]

As shown in Table 1 (entries 1–4), the compositions of the copolymers as determined by ^1H NMR correspond well with those expected from the ratios of the monomer feed. The apparent M_n of the polymers obtained from GPC using PEG calibration, as reported in Table 1, was lower than the M_n calculated from ^1H NMR, which is most likely attributed to the more hydrophilic and molecularly swollen PEG-OH used for GPC calibration than the obtained copolymers. Copolymers obtained by DPP, MSA, and $Sn(Oct)_2$ catalysis (entries 1, 2, and 4, Table 1) displayed highly similar monomodal GPC curves with narrow molar mass distributions ($M_w/M_n < 1.2$) (Figure 3,

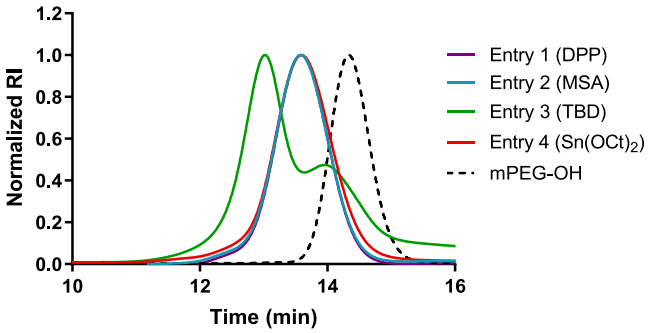

Figure 3. GPC curves of p(CL-*co*-DTC)-PEG block copolymers obtained by the simultaneous copolymerization of CL and DTC at a CL/DTC/mPEG-OH feed molar ratio of 9/4/1 using different catalysts: DPP (entry 1), MSA (entry 2), TBD (entry 3), and $Sn(Oct)_2$ (entry 4). All of the entries presented in the legend correspond to those of Table 1. mPEG-OH (2 kDa) was used as a reference.

purple, cyan, and red lines), suggesting the cross-propagation of both monomers and the absence of side reactions such as transesterification.[9,12,56,57] However, for the copolymer synthesized using TBD as the catalyst (entry 3, Table 1), the GPC curve (Figure 3, green line) showed a broad and bimodal molecular weight distribution. Such a bimodal distribution was previously also observed by the TBD-catalyzed polymerization of a cyclic phosphoester monomer.[58] In our case, the bimodal distribution might be explained by the large difference in monomer reactivity, leading to the inability of homogeneous cross-propagation of both monomers and thus resulting in a highly multidisperse (heterogeneous) composition of the obtained polymer chains.

Considering the advantages of the MSA-catalyzed ROP in terms of the high reaction rate, the lack of residual metal contaminants, mild polymerization conditions, and minimized transesterifications as compared to the other three catalysts, this catalyst was selected for synthesizing p(CL-*co*-DTC)-PEG block copolymers with different compositions (CL with DTC at molar ratios of 9/8 and 18/8) and a p(CL-*co*-DdeTC)-PEG block copolymer at a molar ratio of 9/4 (Scheme 1B). ^1H NMR analysis (Table 1, entries 13–15) shows that these block copolymers were obtained with a high conversion of both monomers and M_n's in close proximity with the expected values. GPC analysis shows that all copolymers prepared by the MSA

https://dx.doi.org/10.1021/acs.macromol.0c01031
Macromolecules 2020, 53, 7009–7024

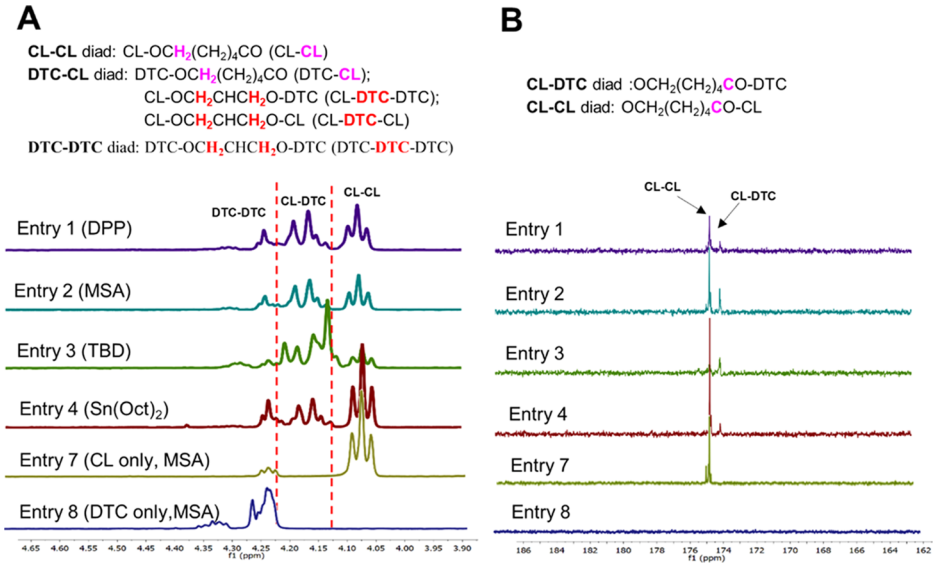

Figure 4. ^{1}H (A) and ^{13}C (B) NMR spectra of p(CL-*co*-DTC)-PEG block copolymers obtained with DPP (entry 1), MSA (entry 2), TBD (entry 3), and Sn(Oct)$_2$ (entry 4) as catalysts, at a CL/DTC/initiator feed molar ratio of 9/4/1. ^{1}H NMR spectra (600 MHz, $CDCl_3$) show the region of methylene protons linked to the oxy-carbonyl group ($C\underline{\boldsymbol{H}}_2OCO$), while ^{13}C NMR spectra (150 MHz, $CDCl_3$) display the region of the caprolactone−carbonyl carbons. The structures of different diads are displayed above the spectra. The reference spectra of block copolymers synthesized using MSA as the catalyst that, besides PEG, only contain CL or DTC blocks are presented as entries 7 and 8, respectively. All of the entries presented in the legend correspond to the same entries in Table 1.

catalysis had narrow molecular weight distributions (M_w/M_n < 1.2), suggesting the absence of the transesterification and termination side reactions, regardless of the feed ratios of the two monomers and the substituent structure of dithiolanes present in the cyclic carbonate-based monomer.

pCL-PEG, pDTC-PEG, and pDdeTC-PEG block copolymers (entries 7, 8, and 16, Table 1), synthesized by the MSA-catalyzed homopolymerization of CL, DTC, or DdeTC using mPEG-OH as an initiator, displayed narrow molecular weight distributions based on the GPC analysis as well (M_w/M_n < 1.1). M_n values according to ^{1}H NMR analysis were all as expected from the monomer/initiator feeds, except for pDdeTC-PEG whose lower M_n relative to that aimed can be explained by the incomplete (75%) conversion of the monomer. Overall, the results of ^{1}H NMR and GPC analyses in Table 1 indicate that MSA is an excellent organocatalyst for the controlled (co)-polymerization of cyclic esters and/or cyclic carbonates.

The different monomer sequences (block, random, or gradient) in the obtained copolymers were determined by ^{1}H/^{13}C NMR analysis, according to the previously described methods.[9,12,13,59] ^{1}H NMR spectra of the different copolymers formed by the simultaneous copolymerization of CL and DTC (Figures 4A and S3A in the Supporting Information) displayed three groups of peaks in the ester region at 4.00−4.30 ppm, corresponding to the three kinds of CH_2O−carbonyl linkages in the different diad structures that are present in the poly(ester carbonate) block (*i.e.*, DTC-DTC, CL-DTC, and CL-CL, respectively).[12,59] In line with these ^{1}H NMR data, the ^{13}C NMR spectra showed two signals in the caprolactone−carbonyl region at 173.5 and 172.9 ppm, which are assigned to CL-CL and CL-DTC diads, respectively (Figures 4B and S3B in the Supporting Information).[13,60,61] DTC-carbonyl peaks in the ^{13}C NMR are located at approximately 155 ppm (not shown), but the intensities of these peaks were relatively low and slightly above noise due to the low amount of DTC used. The peaks are assigned based on the reference spectra of block copolymers synthesized by the MSA catalysis that only contain CL or DTC blocks (presented as entries 7 and 8, respectively, in Figure 4).

The observation that the copolymers synthesized using DPP and MSA as catalysts displayed all diads in the NMR spectra (Figure 4A, entries 1 and 2, and Figure S3 in the Supporting Information) demonstrates a random distribution of CL and DTC in the block copolymers, as can be expected because of the above-discussed similar polymerization kinetics of both monomers. For the p(CL-*co*-DTC)-PEG block copolymer synthesized by the TBD-catalyzed ROP (Figure 4, entry 3), the presence of relatively strong signals at 4.1−4.18 ppm in the ^{1}H NMR spectrum and at 172.9 ppm in the ^{13}C NMR spectrum, being indicative of the link of CL and DTC units (*i.e.*, CL-DTC diads), suggests that the copolymer also had a highly randomized chain structure. This is, however, inconsistent with the expectations based on the substantially different reactivities of the two monomers that were discussed above, strongly indicating that significant transesterification occurred along with chain propagation, as was also indicated by GPC data shown above. For the copolymer obtained using Sn(Oct)$_2$ as catalyst (Figure 4, entry 4), the peak intensities in the ^{1}H NMR spectrum of the CL-CL and DTC-DTC diads were obviously higher and the corresponding CL-DTC diads were lower as compared to those of the corresponding copolymers obtained using DPP and MSA as catalysts. Likewise, an intense signal assigned to CL-CL diads at 173.5 ppm was displayed in the ^{13}C NMR spectrum (Figure 4B, entry 4). Combined with the different polymerization kinetics as observed for the monomers under Sn(Oct)$_2$ catalysis, this indicates the existence of an enriched CL segment in the head of the formed chains and an enriched DTC segment in the tail of the chains and points to the expected gradient microstructure of this copolymer. Obviously, no transesterification occurred, which is in line with our previous publication, where we showed that transesterification in the ROP of CL and (benzylated) hydroxymethyl glycolide using

https://dx.doi.org/10.1021/acs.macromol.0c01031
Macromolecules 2020, 53, 7009−7024

$Sn(Oct)_2$ as catalyst was strongly temperature-dependent and was indeed minimized at 110 °C.[57]

Just like the p(CL-*co*-DTC)-PEG block copolymers discussed above, the p(CL-*co*-DdeTC)-PEG block copolymer (synthesized using MSA as the catalyst) showed the characteristic peaks at 4.00−4.45 ppm in the ^{1}H NMR spectrum, corresponding to CL-CL, CL-DdeTC, and DdeTC-DdeTC linkages, and at 173.6 and 172.8 ppm in the ^{13}C NMR spectrum, corresponding to CL-CL and CL-DdeTC diads (Figure S4 in the Supporting Information). This random monomer sequence is in line with the observed random microstructure of the p(CL-*co*-DTC)-PEG block copolymer obtained under the same reaction condition and also in agreement with the expectation from the comparable reactivities of CL and DdeTC that was observed above.

3.1.2. Copolymers Synthesized by Sequential Ring-Opening Copolymerization of CL with DTC. To investigate the potential of synthesizing p(CL-*co*-DTC)-PEG block copolymers with a blocky monomer order in the hydrophobic block and demonstrate the living nature of the polymerization, sequential copolymerization of CL and DTC initiated by mPEG-OH was performed using MSA or TBD as the catalyst. These catalysts were chosen due to their markedly different catalytic properties in the simultaneous copolymerization process (as discussed in Section 3.1.1). As can be seen from the results (entries 5 and 6, Table 1), in the MSA-catalyzed ROP, regardless of the sequential feeding order of CL and DTC, the conversions of both monomers were quite high (≥97%), and the resulting copolymer compositions based on ^{1}H NMR agreed well with the feed composition and are comparable to those observed with the simultaneous copolymerization of both monomers. ^{1}H NMR analysis in Table 1 clearly shows that the M_n of the block copolymers obtained by sequential copolymerization increased upon feeding of the second monomer. For instance, M_n increased from 2.0 kDa for PEG (entry 17) to 3.0 kDa upon the first polymerization of DTC (entry 8) and then to 4.0 kDa after subsequent copolymerization with CL (entry 6). This is also supported by the GPC analysis (Figure 5A), which showed a continuous peak shift to shorter retention time upon feeding of the first and then the second monomers (*e.g.*, black dotted vs yellow vs blue line), while the molecular weight distributions remained monomodal and narrow (M_w/M_n < 1.1; Table 1). Overall, the results of ^{1}H NMR and GPC analyses suggest that chain extension occurred, emphasizing the living character of the polymerization, resulting in a high level of control with no significant transesterification.

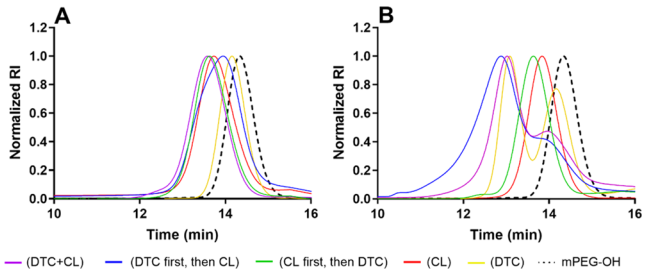

Figure 5. GPC traces of p(CL-*co*-DTC)-PEG block copolymers obtained by the simultaneous and sequential copolymerizations of CL with DTC at a CL/DTC/mPEG-OH feed molar ratio of 9/4/1, using MSA (A) and TBD (B) as the catalysts. Purple lines represent the block copolymers obtained by the simultaneous copolymerization of CL and DTC, corresponding to entries 2 and 3 in Table 1; the blue lines represent the block copolymers obtained by the sequential polymerization of DTC first, followed by CL, corresponding to entries 5 and 9 in Table 1; the green lines represent the block copolymers obtained by the sequential polymerization of CL first and then DTC, corresponding to entries 6 and 10 in Table 1; and the red and yellow lines represent pCL-PEG and pDTC-PEG obtained by homopolymerization of either CL or DTC, corresponding to entries 7, 11 (the former) and 8, 12 (the latter) in Table 1.

With TBD as the catalyst, and when the sequential polymerization of the comonomers was performed in the order of DTC first followed by CL (entry 9, Table 1), the composition of the obtained block copolymer based on ^{1}H NMR analysis agreed with the feed composition with almost complete conversions of both monomers. However, from the GPC analysis (Figure 5B), it can be seen that the thus prepared block copolymer had a broad bimodal molecular weight distribution (blue line) with a polydispersity index of 1.31 in line with that obtained by the simultaneous copolymerization of the comonomers (purple line). This phenomenon has been previously reported for copolymers synthesized by the sequential polymerization of TMC first, followed by CL at a 50/50 molar ratio using yttrium isopropoxide catalysis (M_w/M_n = 3.7), which was attributed to a relatively slow ring opening of CL by the living poly(TMC) chain end in comparison to the CL polymerization by living CL growing ends.[12] However, in our case, pDTC-PEG synthesized under the same condition also displayed a bimodal molecular weight distribution (Figure 5B, yellow line), indicating that the highly multidispersity in the copolymer composition occurred already in the initiation step. This suggests that not all of the potentially active groups (OH) of mPEG-OH in the reaction mixture acted as an initiator of the polymerization since one of the GPC peaks partly overlapped with mPEG-OH. This may be attributed to the fast ring opening of DTC along with fast chain growth (*i.e.*, propagation rate ≥ initiation rate), which was also observed for the TBD-catalyzed simultaneous copolymerization of CL and DTC presented in Section 3.1.1. However, in contrast, homopolymerization of CL under TBD catalysis is likely characterized by a relatively fast reaction of the PEG terminal OH with the monomers followed by relatively slow propagation, thus leading to block copolymers with narrow molecular weight distribution (M_w/M_n = 1.03−1.05), as indicated by the GPC analysis of pCL-PEG obtained by both TBD and MSA-catalyzed ROP (Figure 5, red lines, entries 7 and 11).

For the copolymer synthesized by the TBD-catalyzed ROP of CL first, followed by DTC (entry 10, Table 1), the composition and M_n calculated by ^{1}H NMR of the final block copolymer still well matched with the expected values based on the monomer/initiator ratios. ^{1}H NMR analysis shows that the M_n of the block copolymer was comparable to that prepared by MSA catalysis, *i.e.*, increasing from 2.0 kDa for PEG (entry 17) to 3.2 kDa after the first polymerization of CL (entry 11), and then to 4.0 kDa after the polymerization of DTC in the second step (entry 10). In line with this, the GPC analysis showed a similar trend of increasing M_n in the first and second steps, respectively (Figure 5B, black dotted vs red vs green line), while a monomodal molecular weight distribution of the final block copolymer remained as narrow as its control pCL-PEG (M_w/M_n < 1.1) (green vs red line). This indicates that the formation of multidisperse copolymers can be avoided by first polymerizing the slowly propagating CL (initiation rate > propagation rate) to produce living CL growing chain ends (Figure 5B, red line), followed by polymerization with DTC (Figure 5B, green line).

https://dx.doi.org/10.1021/acs.macromol.0c01031
Macromolecules 2020, 53, 7009−7024

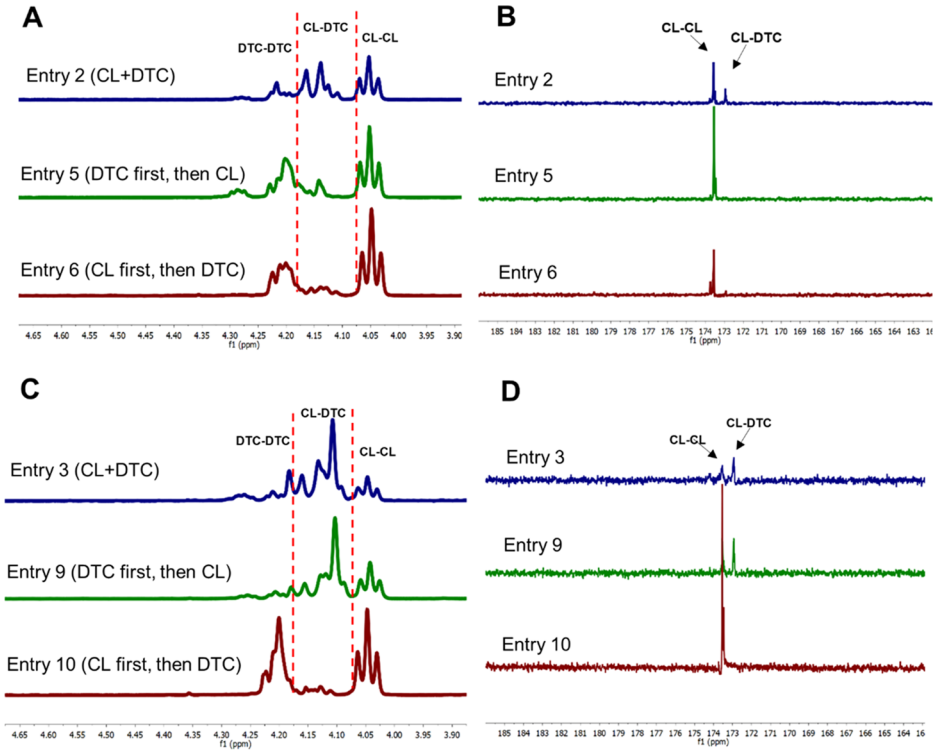

Figure 6. ^{1}H (A, C) and ^{13}C (B, D) NMR spectra of p(CL-*co*-DTC)-PEG block copolymers obtained by the simultaneous and sequential copolymerizations of CL and DTC at a CL/DTC/mPEG-OH feed molar ratio of 9/4/1, using MSA (A, B) and TBD (C, D) as the catalysts, respectively. ^{1}H NMR spectra (600 MHz, $CDCl_3$) show the region of methylene protons linked to the oxy-carbonyl group ($C\underline{\boldsymbol{H}}_2OCO$), while ^{13}C NMR spectra (150 MHz, $CDCl_3$) display the region of the caprolactone−carbonyl carbons. Entries 2 and 3 were obtained by the simultaneous polymerization of CL and DTC. All of the entries correspond to the same entries in Table 1.

^{1}H/^{13}C NMR analysis was used to determine the monomer sequence of the obtained block copolymers. Using MSA as catalyst (Figure 6A,B, entries 5 and 6), the block copolymers prepared by the sequential copolymerization of CL and DTC, regardless of the feed order, had minor signals of the link between CL and DTC units (*i.e.*, CL-DTC diads) but displayed increased signals attributed to the presence of the CL-CL and DTC-DTC blocks as compared to the polymer obtained by simultaneous copolymerization (*i.e.*, entry 2 in Figure 6A,B). These results strongly indicate highly blocky structures of the polyester/carbonate block of the formed p($CL_{9.1}$-*b*-$DTC_{4.1}$)-PEG and p($DTC_{3.8}$-*b*-CL_9)-PEG (entries 5 and 6, Table 1) block copolymers with no signs of transesterification that would randomize the monomer sequence. In the case of TBD catalysis, however, for the block copolymer obtained by polymerization of DTC first followed by CL, the presence of CL-DTC diads in the δ 4.10−4.18 ppm region and at 172.9 ppm of the ^{1}H and ^{13}C spectra, respectively (Figure 6C,D, entry 9), indicate random CL and DTC sequences, with relative peak intensities as high as that observed in the NMR spectrum of the polymer obtained by the simultaneous copolymerization of CL and DTC (*i.e.*, Figure 6C,D, entry 3). These results suggest that copolymerization of DTC first followed by CL yielded a random copolymer, most likely due to the occurrence of substantial transesterification. However, the NMR signals in the CL-DTC diad regions were hardly observed in the spectra when the copolymer was synthesized by reverse feeding of the monomers (*i.e.*, CL first, followed by DTC), while the increased signals assigned to CL-CL and DTC-DTC linkages do indicate a blocky structure (Figure 6C,D, entry 10).

Previously, it was reported that the sequential copolymerization of CL and a functionalized TMC (the feeding order of both monomers was not reported) using TBD as the catalyst with a monomer-to-initiator ratio of 80/80/1 indeed produced a random copolymer due to transesterification.[9] Also, such chain reshuffling reactions were observed with the sequential copolymerization of L-lactide and TMC using 1,8-diazabicyclo[5.4.0]undec-7-ene (DBU) as the catalyst.[11] The incidence of these side reactions is most likely because the carbonate ester bonds in the DTC-DTC linkages (formed when DTC was polymerized first) are not as stable as the ester bonds in DTC-CL or CL-CL diads and could react intra- or intermolecularly with propagating the hydroxyl chain ends. When the more stable ester bonds were formed first, which is the case of the ROP of CL first, the subsequently added DTC was not able to break the formed ester bonds, thus resulting in prevailing chain propagation with negligible transesterification reactions.

3.2. Thermal Properties of the Copolymers. The thermal properties of the obtained block copolymers were investigated by DSC (results are summarized in Table 1). Only one T_m at 40−45 °C close to that of mPEG-OH (48 °C) was detected, which is in accordance with the previous data.[62,63] For the obtained p(CL-*co*-DTC)-PEG and p(CL-*co*-DdeTC)-PEG block copolymers, degrees of crystallinities (*i.e.*, ΔH_m) of PEG corrected for its weight fraction in the corresponding block copolymers (Figure S5A, Supporting Information) were in good agreement with that of the mPEG-OH (182 J/g, entry 17, Table 1), demonstrating that these block copolymers were phase-separated in the solid state in crystalline PEG domains and amorphous p(CL-*co*-DTC) or p(CL-*co*-DdeTC) domains with

https://dx.doi.org/10.1021/acs.macromol.0c01031
Macromolecules 2020, 53, 7009−7024

T_g's ranging from −47 to −11 °C. These amorphous domains are obviously not miscible with PEG. It is noted that the T_g's of p(CL-*co*-DTC)-PEG and p(CL-*co*-DdeTC)-PEG block copolymers with a random distribution of CL and DTC or DdeTC as confirmed by NMR analysis and discussed in Section 3.1 (*i.e.*, entries 1−3, 9, and 13−15, Table 1) can indeed be described by the Fox equation (see Figure S5B, Supporting Information). The pCL-PEG block copolymers (entries 7 and 11, Table 1) were almost fully crystalline: both PEG and pCL have their T_m around 45 °C,[63] while the pDTC-PEG (entry 8, Table 1) and pDdeTC-PEG (entry 16, Table 1) block copolymers had crystallinity from PEG and amorphous pDTC and pDdeTC domains with T_g's at −6.3 and −17 °C, respectively.

3.3. Effect of Reducing Agents on the Dynamic Crosslinking Properties of Micelles. The capability of dithiolanes in DTC units to crosslink nanoparticles has been reported in previous studies.[29,31,32] In the present work, DTC units were successfully introduced to PEG-poly(ε-caprolactone)-based block copolymers, as discussed in Section 3.1, and therefore, the reduction of the dithiolanes present in these block copolymers by different reducing agents was investigated. For this purpose, micellar dispersions were prepared from the p(CL_{18}-$DTC_{7.5}$)-PEG block copolymer with a random monomer order in the hydrophobic block (*i.e.*, entry 14, Table 1) at a final polymer concentration of 4 mg/mL using a nanoprecipitation method. The obtained micelles dispersed in PBS were subsequently incubated with reducing agents that had none, one, or two thiol moieties (*i.e.*, TCEP, GSH, or DTT, respectively) at molar ratios to dithiolanes varying from 0 to 2 at 37 °C. The ring opening of the dithiolane groups by the reduction of the disulfide bonds by the reducing agent (RA) was monitored by recording the changes in the absorbance of DTC at 326 nm.[38,42] Figure 7A shows that the incubation of micelles with TCEP and DTT for 1 h caused an RA concentration-dependent linear decrease in the absorbance of the micellar dispersions at 326 nm, up to 1 equiv of RA, clearly indicating that these RAs were able to cleave the disulfide bonds in the dithiolane rings of DTC units to free thiol groups. It is noted that a prolonged incubation (up to 40 h) did not result in a further decrease of the absorbance, and thus, the formed sulfhydryls were preserved in a reduced state for at least 40 h in the presence of the RA. In line with this, Ellman's assay demonstrated the quantitative formation of free thiol groups in the micellar dispersions with series of molar ratios of TCEP to dithiolanes (Figure S6, black dots, Supporting Information). In contrast, in the presence of GSH, no change in the absorbance at 326 nm was observed for the p(CL_{18}-$DTC_{7.5}$)-PEG micellar dispersion even after the addition of a 2-fold equivalent of GSH and incubation for 58 h (Figure 7A, blue line). This indicates that the dithiolane rings remained intact, meaning that the reductive capacity of GSH was too low to break the disulfide bonds in dithiolanes. The fact that GSH is a less strong reducing agent than TCEP and DTT has been reported in other papers.[64,65]

In the second step, to crosslink the reduced micelles, the reducing agent was removed by dialysis, during or after which (intra- or intermolecular) disulfide bonds can be formed by oxidation in the air. To follow this process, the absorbance of the reduced micelles at 326 nm was monitored over time after removing the reducing agents by dialysis. For p(CL_{18}-$DTC_{7.5}$)-PEG micelles preincubated with TCEP or DTT, the absorbance of DTC units was similar or slightly lower directly after dialysis as compared to the corresponding values before dialysis (the colored symbols in Figure 7B,C; "AD + 0 h" vs "BD"). However,

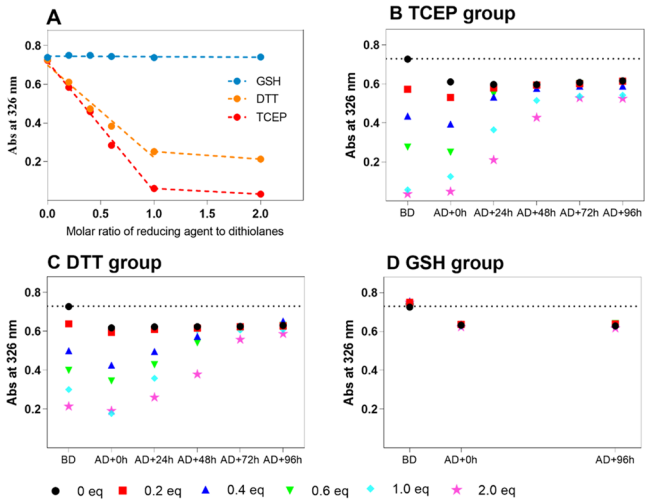

Figure 7. (A) Dithiolane absorbance (Abs) at 326 nm in micellar dispersions consisting of p(CL_{18}-$DTC_{7.5}$)-PEG (entry 14, Table 1) in response to different reducing agents in PBS (pH 7.4) at 37 °C, 1 h after the addition of various amounts of TCEP (red line), DTT (orange line), or GSH (blue line). (B−D) Absorbance (Abs) of p(CL_{18}-$DTC_{7.5}$)-PEG (entry 14, Table 1) micellar dispersions at 326 nm in time before and after dialysis; micellar dispersions at polymer concentrations of 4 mg/mL in PBS/DMF (9/1 v/v) were incubated with different reducing agents, TCEP (B), DTT (C), and GSH (D), at various amounts (shown by the different symbols) for 7 h at 37 °C and then dialyzed against PBS for 12 h, while the absorbance of these micellar dispersions was recorded before dialysis (BD), directly after dialysis (presented as "AD + 0 h"), and at different time points after dialysis.

the absorbance increased slowly when exposed to air in PBS at RT for a prolonged time ("AD + 24 h" to "AD + 96 h" in Figure 7B,C), to finally reach the same level as for the micelles that were not exposed to an RA (*i.e.*, black dots). The final absorbance value of ∼0.6 corresponds to an ∼20% change compared to the absorbance measured directly after preparation of the micelles and in the absence of RA (∼0.75). In line with these results, Ellman's assay of the TCEP-reduced micelles (Figure S6, Supporting Information) shows that the concentration of sulfhydryls in the micellar dispersion before and after dialysis was comparable (black vs red dots) but decreased to a negligible concentration during 4 days' aging after dialysis (blue dots). Also, the appearance of a peak at an 11 min retention time in GPC traces of these micelles shows that crosslinking of micelles occurred between 0 and 96 h aging after dialysis (the solid lines in Figure S7A,B, respectively, Supporting Information). These results suggest that free thiols present in the micelles, obtained by the cleavage of the dithiolanes using a reducing agent, slowly oxidized in time after dialysis and preferably (∼80%) returned to its original state of five-member dithiolanes, while a minority of them (max. ∼20%) formed new and intermolecular disulfide bonds.

As indicated in Figure 7B−D by the black dots, for the p(CL_{18}-$DTC_{7.5}$)-PEG micelles without pretreatment with RA, the absorbance dropped from approximately 0.75 to 0.60 during dialysis. After dialysis, the absorbance did not change further when kept in PBS for 96 h. As expected, Figure 7D shows that p(CL_{18}-$DTC_{7.5}$)-PEG micelles that were incubated with GSH (colored symbols) gave the same results as for micelles that were not treated with any RA (black dots), due to the insufficient reduction power of GSH as mentioned above.[64,65] In the GPC

https://dx.doi.org/10.1021/acs.macromol.0c01031
Macromolecules 2020, 53, 7009−7024

chromatograms of the p(CL_{18}-$DTC_{7.5}$)-PEG block copolymer after dialysis without pretreatment with RA (the red dotted line in Figure S7A of the Supporting Information), the peak height of the original polymer at ∼13 min reduced and a new peak appeared at a higher molecular weight (retention time of ∼11 min), while the total area under the curve remained almost similar. The relative molecular weight of the new peak (*i.e.*, 13 kDa) suggests that approx. 4 polymer chains are connected, which is lower than expected for a fully crosslinked micelle. Although the absolute molecular weight (and thus the number of connected polymers) may be higher, this is probably the result of the relatively low crosslink density (20%) and dynamic nature of the crosslinking, causing that some loosely connected polymer chains are de-crosslinked when dissolved in DMF. Overall, these results suggest that approximately 20% of the dithiolane rings were spontaneously (*i.e.*, without being triggered by an RA) converted during dialysis into intermolecular bonds by disulfide exchange (probably a radical process), which in turn resulted in crosslinking of the core of the micelles. In line with this, it has been reported that p(TMC_{190}-DTC_{25})-PEG polymersomes[32,66] and cRGD/TAT-conjugated p($CL_{17.5}$-$DTC_{5.2}$)-PEG micelles spontaneously crosslinked after dialysis due to the presence of dithiolanes.[31] These nanoparticles showed complete disappearance of dithiolanes after dialysis by the UV/vis, indicating that their crosslink densities were much higher than those of p(CL_{18}-$DTC_{7.5}$)-PEG micelles in our work. The driving force for the spontaneous formation of the disulfide-crosslinked network during the dialysis process is probably the removal of the remaining organic solvent (10% DMF after the nanoprecipitation), resulting in condensation of the core of micelles, bringing the dithiolanes in the core in close vicinity to each other to allow disulfide exchange reactions to proceed.[29]

The obtained results demonstrate that the disulfides in micelles derived from dithiolanes have dynamic properties. Its redox state (e.g., the number of free thiols) can be influenced by the addition of an RA, but the final equilibrium state in the absence of an RA (*i.e.*, the ratio between the intramolecular and intermolecular disulfide bonds) is not affected by preincubation with an RA. Thus, the RA in fact acts as a catalyst that accelerates the reduction of dithiolane but does not affect the final thermodynamic equilibrium.

3.4. Effect of the Monomer Sequence on the Dynamic Crosslinking Properties of Micelles. To investigate whether the different CL and DTC sequences in the hydrophobic blocks of the copolymers have an effect on the dynamic properties of dithiolane-based crosslinking, we selected three different copolymers synthesized by the MSA-catalyzed ROP (see Section 3.1) that had similar chain lengths of hydrophobic blocks (9 units of CL and ∼4 units of DTC) but differed in the order of CL and DTC units in the hydrophobic blocks, *i.e.*, random p(CL_9-$DTC_{3.9}$)-PEG (entry 2, Table 1) or blocky p($CL_{9.1}$-*b*-$DTC_{4.1}$)-PEG (entry 5, Table 1) and p($DTC_{3.8}$-*b*-CL_9)-PEG (entry 6, Table 1). These micelles showed the same changes in absorbance at 326 nm as observed above with the p(CL_{18}-$DTC_{7.5}$)-PEG micelles, *i.e.*, a decreasing absorbance upon exposure to TCEP or DTT (before dialysis) and increasing during aging after dialysis, as can be seen from Figures S8−S10 (Supporting Information). The rate of a five-member dithiolane recovery after dialysis was faster than that observed for p(CL_{18}-$DTC_{7.5}$)-PEG micelles with a random monomer order in the hydrophobic block; however, the final equilibrium was not shifted by the shorter chain lengths of the hydrophobic polyester/carbonate block and was independent of the CL and DTC orders in the hydrophobic blocks of the p(CL-*co*-DTC)-PEG block copolymers.

3.5. Effect of the Nature of Dithiolane Unit on the Dynamic Crosslinking Properties of Micelles. The preference to reform intramolecular disulfide bonds (*i.e.*, five-member dithiolane rings) rather than new intermolecular disulfide bonds in p(CL-*co*-DTC)-PEG-based micelles, as shown above, may be influenced by the distance between the pendant sulfur groups and the backbone of the polymer chains, *i.e.*, the nature of dithiolane units in the polymer chains. To verify this hypothesis, random p(CL_9-$DdeTC_{3.1}$)-PEG (entry 15, Table 1) containing ethylene glycol diester as a flexible spacer between the dithiolane groups and backbone of the polymer chains was used to prepare micellar dispersions with/without TCEP or DTT at a polymer concentration of 10 mg/mL.

In line with DTC-based micelles described in Sections 3.3 and 3.4, the addition of TCEP to the micellar dispersions triggered the reduction of disulfide bonds in DdeTC units within 1 h to a different extent and dependent on the TCEP concentration (Figure S11A,C, Supporting Information), but reduction by DTT took longer (5 h: Figure S11B). Remarkably, the absorbance at 328 nm of p(CL_9-$DdeTC_{3.1}$)-PEG micelles without being preincubated with RA did not decrease during and after dialysis (Figure 8A,B, black dots). In line with this,

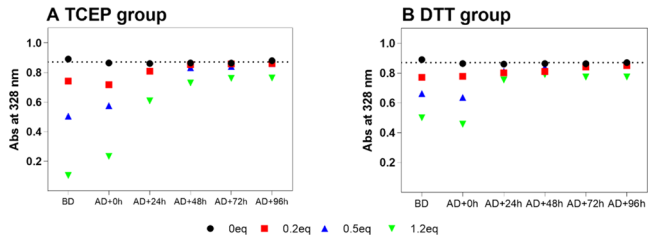

Figure 8. Absorbance (Abs) of DdeTC in micellar dispersions consisting of 10 mg/mL p(CL_9-$DdeTC_{3.1}$)-PEG (entry 15, Table 1) at 328 nm. Dispersions were incubated with 0−1.2 equiv (shown by the different colors) of reducing agent TCEP (A) or DTT (B) for 7 h at 37 °C, dialyzed against PBS for 12 h and then aged for 96 h; the absorbance of the dispersions was recorded before dialysis ("BD"), directly after dialysis ("AD + 0 h"), and at different time points during aging after dialysis ("AD + *X* h").

GPC profiles of these p(CL_9-$DdeTC_{3.1}$)-PEG micellar dispersions (not preincubated with an RA and after dissolution in DMF) obtained before, directly after dialysis, and 96 h aging after dialysis were identical to that of the original p(CL_9-$DdeTC_{3.1}$)-PEG block copolymer (Figure S12, red vs gray dotted lines, Supporting Information), demonstrating that spontaneous crosslinking of the micelles by disulfide exchange did not occur during dialysis, as opposed to the DTC-containing micelles. In addition, DLS measurements demonstrate that both non-crosslinked control pCL_9-PEG and p(CL_9-$DdeTC_{3.1}$)-PEG micelles fully dissolved in DMF, indeed suggesting that no disulfide-crosslinked network was present in the micelles.

It was observed that for DdeTC-containing micelles preincubated with either TCEP or DTT, the reduced absorbance at 328 nm upon incubation with the RA gradually reversed toward the starting values over the course of 48 h after dialysis (Figure 8, red, blue, and green dots). Considering the experimental error, the equilibrium values (∼0.83) were close to those observed in micellar dispersions without being preincubated with an RA (∼0.87), indicating that the majority of free thiols in the reduced p(CL_9-$DdeTC_{3.1}$)-PEG micelles returned

https://dx.doi.org/10.1021/acs.macromol.0c01031
Macromolecules 2020, 53, 7009−7024

to its original five-member dithiolane rings upon oxidation during aging. In line with this, GPC curves from these micelles obtained 96 h after dialysis (Figure S12C, solid lines, Supporting Information), showed only a small shoulder in the chromatogram at about 11 min, corresponding to the crosslinked micelles. Overall, these results suggest that the ability to crosslink micelles containing dithiolanes of DdeTC units was much lower than that of DTC. In other words, inserting a flexible spacer between dithiolanes and the backbone of the polymer chains does, unexpectedly, not favor the crosslinking capacity of dithiolanes in micelles. This could be ascribed to a slightly different ring tension between DTC and DdeTC or electronic induction effects caused by the different substitution pattern on the dithiolane ring.[67−69] In addition, these observations are inconsistent with those reported in previous studies, in which it was shown that pDdeTC-PEG-pDdeTC triblock copolymers self-assembled in water into bridged flower-like micelles, which in turn efficiently crosslinked through ring-opening polymerizations of the dithiolanes initiated by the addition of a thiol.[37,40,42] These and our studies differ in the experimental setup and composition of the copolymers used. To exclude the possible impact of the former on the result, we repeated the same method as reported in ref 42 (described in Figure S13, Supporting Information), *i.e.*, direct hydration of p(CL_9-$DdeTC_{3.1}$)-PEG (entry 15, Table 1) and $pDdeTC_5$-PEG (entry 16, Table 1), to reach polymer concentrations of 10 and 20 mg/mL, respectively, followed by ring-opening polymerization of the dithiolanes initiated by 3,6-dioxa-1,8-octanedithiol and thiol capping by maleimide. As indicated by the decrease of the absorbance of DdeTC units at 328 nm in Figure S13A,B (Supporting Information), 3,6-dioxa-1,8-octanedithiol was indeed able to reduce the dithiolanes in p(CL_9-$DdeTC_{3.1}$)-PEG dispersions to some extent within 1 h (Figure S13A, red dots, Supporting Information), while the reduction of $pDdeTC_5$-PEG dispersions took 3 h (Figure S13B, red dots, Supporting Information). It is noted that the absorbance of the dithiolanes in these micelles could not be monitored after being capped by maleimide due to the interference of maleimide absorbance with that of DdeTC. However, both reduced dispersions, regardless of being capped with maleimide or not, showed the same GPC curves as the corresponding original p(CL_9-$DdeTC_{3.1}$)-PEG and $pDdeTC_5$-PEG polymers (Figure S13C,D, Supporting Information). Neither a peak nor a shoulder was observed at a retention time of 11 min, suggesting that under the same condition as reported previously,[42] the DdeTC-containing micelles were not able to be crosslinked through ring-opening polymerization of dithiolanes. The inconsistency between our and literature data might be ascribed to the slightly different polymer structures and compositions, even though such a big difference in crosslinking behavior between triblock $pDdeTC_4$-PEG(20 kDa)-$pDdeTC_4$ and diblock $pDdeTC_5$-PEG(2 kDa) with shorter PEG chains was unexpected.

3.6. Reversibility of the Crosslinking in Micelles. The reversibility of the crosslinking (or the reformed cyclic dithiolanes) in micelles that were aged for 96 h after TCEP reduction and dialysis (represented by the red box in the inset of Figure 9, denoted as the first cycle) was investigated using p(CL_{18}-$DTC_{7.5}$)-PEG (entry 14, Table 1). The aged micelles were therefore re-incubated with TCEP for 7 h using various molar ratios to the dithiolanes (designated as the second cycle in Figure 9). As expected, for the p(CL_{18}-$DTC_{7.5}$)-PEG micelles not treated with TCEP in the second cycle, the absorbance of DTC at 326 nm did not change during the whole process of

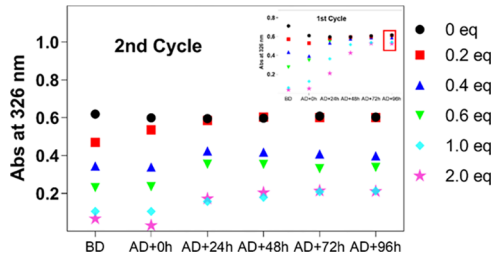

Figure 9. Absorbance (Abs) of micellar dispersions composed of p(CL_{18}-$DTC_{7.5}$)-PEG (entry 14, Table 1) at 326 nm after a second exposure to various amounts (indicated by the different symbols) of TCEP for 7 h at 37 °C (presented as "BD"), after subsequent dialysis (presented as "AD + 0 h"), and upon aging after dialysis for the indicated time points; micellar dispersions were used from the first cycle after 96 h of aging, as indicated by the red box in the inset copied from Figure 7B.

second-time dialysis and aging, indicating that the crosslinked core of micelles remained intact with constant crosslinking density, which is further confirmed by the similar GPC traces of micelles obtained after first and second cycles of nonreducing conditions (Figure S7, red line, vs Figure S14C, black line, respectively). Upon the addition of various amounts of TCEP in the second cycle, the absorbance of DTC in these micelles at 326 nm (at "BD" in Figure 9) showed a TCEP concentration-dependent decrease, which was consistent with that shown in the first cycle, meaning that the reformed dithiolane rings in the micelles in the first cycle were reversibly cleaved under reductive conditions (TCEP), as expected.

The absorbance values of the p(CL_{18}-$DTC_{7.5}$)-PEG micelles treated with 0.2 equiv of TCEP and after dialysis recovered within 24 h from 0.47 to the starting level of 0.6, which was comparable to the level observed for micelles incubated without TCEP (Figure 9, red vs black dots). Interestingly, when micelles had been incubated with ≥0.4 equiv of TCEP, the absorbance values of micelles increased slowly during aging but did not reach the same plateau at 0.6 (see Figure 9). Also, Ellman's assay showed that the number of free thiols in those micelles obtained 96 h after dialysis in the second cycle was higher than that of the micelles from the first cycle (Figure S6, pink vs blue dots). This suggests that the reduced dithiolane rings and/or crosslinking in micelles caused by relatively high amount of TCEP were not completely reversed to its original stage, as shown in the first cycle under the same condition. DLS measurements show that the p(CL_{18}-$DTC_{7.5}$)-PEG micelles preincubated without or with 0.2 equiv of TCEP in the second cycle displayed a constant and comparable size and derived count rate before dialysis, as well as directly after dialysis and 96 h aging after dialysis (Figure S14A,B in the Supporting Information, red and black lines). However, micelles exposed ≥0.4 equiv of TCEP in the second cycle exhibited a significant decrease in size (from 23 to 10 nm) and the derived count rate (from 8000 to 2000) during and after dialysis (Figure S14A,B, blue, green, light green, and pink lines). GPC chromatograms show that these p(CL_{18}-$DTC_{7.5}$)-PEG micelles obtained after the second cycle (Figure S14C, blue, green, light green, and pink lines, Supporting Information) displayed a decrease of the main peak at a retention time of approximately 13 min and the appearance of a new peak at a higher retention time (about 14.5 min), most likely attributed to hydrolyzed fragments of the diblock copolymer. In addition, the ^{1}H NMR spectrum of the micelles pre-exposed to 1 equiv of TCEP in the second cycle (Figure S15 in the Supporting

https://dx.doi.org/10.1021/acs.macromol.0c01031
Macromolecules 2020, 53, 7009−7024

Information) shows that the degree of polymerization of DTC and CL decreased from 7.5 to 1.4 and 18 to 11.5, respectively, suggesting that the hydrolysis of polymers indeed occurred in the micelles. Thus, the incomplete reversibility of dithiolane ring formation and/or crosslinking in the case of the micelles preincubated with a high amount of TCEP can be explained by the loss of DTC units. This accelerated hydrolysis is probably caused by the formation of a cyclic eight-member carbonate between C═O (as the H-bond acceptor) in the backbone and the large amount of adjacent free sulfhydryls (as the H-bond donor) formed by a high amount of TCEP. This hydrolysis likely also occurred in the first cycle but to a lower extent than that observed in the second cycle due to the relatively shorter storage period of those micelles in PBS in the first circle as compared to that in the second cycle (4 and ∼9 days, respectively).

3.7. De-Crosslinking of Micelles. As shown in previous sections, DTC-containing micelles, but not DdeTC-based micelles, spontaneously crosslinked during dialysis, to the same extent as with previous exposure to an RA. To evaluate the cleavage of the disulfide crosslinks in the former micelles in more detail, several spontaneously crosslinked p(CL-*co*-DTC)-PEG-based micelles (entries 2, 6, 13, and 14, Table 2) were prepared without exposure to an RA, *i.e.*, by the dropwise addition of the polymer solution in DMF to PBS (pH 7.4) at a volume ratio of 1:9 followed by dialysis against PBS for 12 h. GPC curves (Figure S16 in the Supporting Information) and the decrease of the absorbance of DTC at 326 nm before and after dialysis (Table 2) suggest that indeed crosslinked micelles were formed spontaneously after dialysis with about an ∼20% crosslinking density, as reported in Sections 3.3 and 3.4. It is worth noting that micelles with a higher DTC-to-CL comonomer ratio in the hydrophobic polyester/carbonate blocks (entry 13, Table 2) had similar crosslink density (*i.e.*, absorbance change) after dialysis as those with a lower DTC-to-CL ratio (entries 2 and 14, Table 2), suggesting that the density of the crosslinkable units was not a determinant factor for the final equilibrium ratio between intra- and intermolecular disulfide bonds within the range of ratios studied here. In addition, as shown in Table 2, all prepared micelles had average diameters ranging from 17 to 21 nm with narrow PDIs in PBS.

Table 2. Characteristics of Spontaneously Crosslinked Micelles Prepared from Different Polymers at a Polymer Concentration of 4 mg/mL

entry[a]	polymers	*Z*-ave (nm)[b]	PDI	absorbance change[c]
2	p(CL_9-$DTC_{3.9}$)-PEG	18 ± 1	0.11 ± 0.03	18 ± 2%
6	p($DTC_{3.8}$-*b*-CL_9)-PEG	18 ± 1	0.10 ± 0.05	18 ± 2%
9	pCL_9-PEG	17 ± 1	0.15 ± 0.06	n.a.[d]
13	p(CL_9-$DTC_{6.6}$)-PEG	18 ± 0	0.07 ± 0.02	17 ± 3%
14	p(CL_{18}-$DTC_{7.5}$)-PEG	22 ± 2	0.09 ± 0.02	20 ± 2%

[a]Entries in this table correspond to those listed in Table 1. [b]*Z*-average diameter of the micelles in PBS was measured by DLS after nanoprecipitation and dialysis (n = 3). [c]Relative decrease in absorbance at λ = 326 nm. [d]Not applicable.

The non-crosslinked control pCL_9-PEG micelles were capable of dissolving in DMF, as apparent from the loss of scattering intensity by DLS upon dilution in DMF (Figure S17 in the Supporting Information). In contrast, scattering intensities (*i.e.*, derived count rates) of spontaneously pre-crosslinked p(CL-*co*-DTC)-PEG-based micelles decreased just slightly when incubated with DMF (Figure 10C, blue vs black columns), while the size increased from approximately 20 nm to around 30−90 nm depending on the molecular weight (*i.e.*, the chain lengths of hydrophobic blocks) and the PDIs remained <0.3 (Figure 10A,B, blue vs black columns). These observations suggest that DTC-containing micelles were indeed stabilized, *i.e.*, did not disassemble completely but swelled when dispersed in DMF, due to the existence of core crosslinkages in the micelles. The decreased scattering intensity could be explained by either the decreased refractive index (RI) increment (dn/dc) resulting from swelling of the micelles or the micelles partly dissociated in DMF, most likely due to the dynamic and labile disulfide bonds and relatively low crosslinking density in the core of micelles. Interestingly, spontaneously pre-crosslinked p(CL-*co*-DTC)-PEG micelles did dissolve when incubated with TCEP in PBS followed by the addition of an excess of DMF, as indicated by negligible scattering measured by DLS. These data suggest that indeed the disulfide crosslinks formed by dithiolanes in the core of micelles were reversibly destroyed in the presence of a reducing agent (*i.e.*, TCEP), leading to complete dissociation of micelles in DMF.

In addition, the de-crosslinking potential of different reducing agents (TCEP, DTT, and GSH) toward dithiolane-crosslinked micelles was evaluated by GPC analysis. Therefore, crosslinked p(CL_{18}-$DTC_{7.5}$)-PEG micelles (entry 14, Table 2) were incubated with 10 mM DTT, TCEP, or GSH at 37 °C. The resulting chromatograms (Figure 10D, red, blue, and green lines) were identical to the starting p(CL_{18}-$DTC_{7.5}$)-PEG block copolymer (Figure 10D, black line), suggesting that the crosslinked micelles were fully reduced (*i.e.*, de-crosslinked) in the reductive environment at physiological temperature and redox potential (10 mM GSH is equal to the intracellular concentration[24]). In other words, all of these three reducing agents, including the physiological GSH, were capable of cleaving the linear disulfide crosslinking present in the core of micelles. This is surprising since the reducing ability of GSH was too weak to reduce the disulfide bonds present in the cyclic dithiolanes (see Section 3.3) but apparently sufficient to break the crosslinks, which suggests that the cyclic dithiolanes are more stable than the newly formed linear disulfide bonds in micelles after dialysis. This also explains to some extent why free thiols produced by the reduction of dithiolanes tend to reform five-member dithiolanes during dialysis and aging rather than forming or keeping the crosslinks.

4. CONCLUSIONS

Poly(ε-caprolactone)-based polymeric micelles that are under investigation for drug delivery applications can be made self-crosslinkable by introducing dithiolane rings directly connected to the backbone. On the other hand, introduction of a linker unit between the dithiolane and the backbone prevents crosslinking, probably because of a different ring strain and/or electronic substituent effects. This crosslinking of micelles by disulfide exchange occurs spontaneously when the organic solvent (DMF) is removed during dialysis after nanoprecipitation and is independent of the monomer sequence (*i.e.*, random or blocky) in the hydrophobic blocks or CL/DTC ratio of the block copolymers or addition of reducing agents. Regarding the synthesis of the copolymers, we have shown that different catalyst types, *i.e.*, acidic (DPP or MSA), basic (TBD), or

https://dx.doi.org/10.1021/acs.macromol.0c01031
Macromolecules 2020, 53, 7009−7024

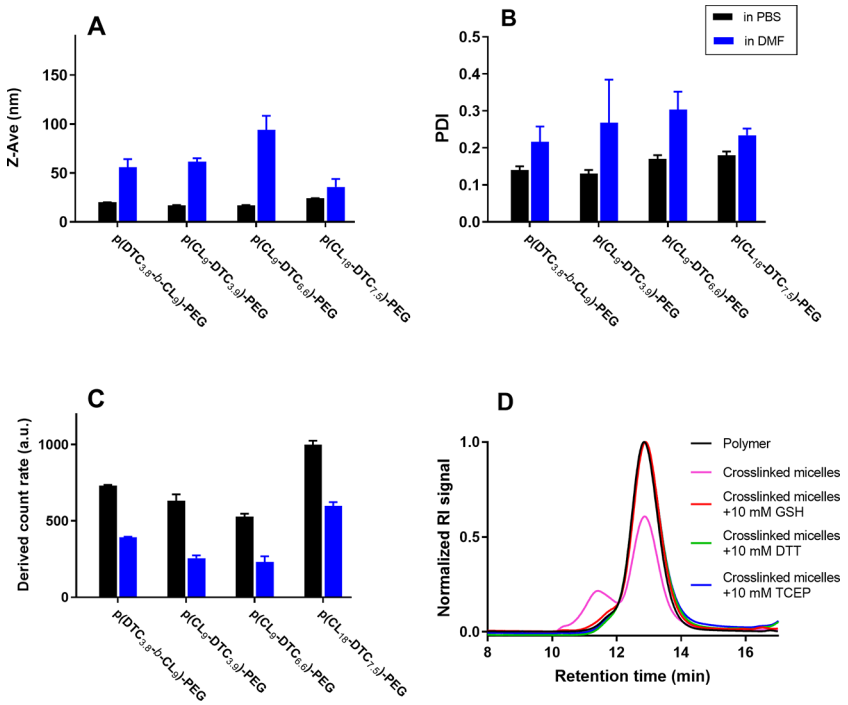

Figure 10. (A–C) Size (A), polydispersity index (PDI) (B), and derived count rate (C) of spontaneously crosslinked micellar dispersions composed of p(CL-*co*-DTC)-PEG-based polymers (entries 2, 6, 13, and 14, Table 2) determined by DLS, after dilution in DMF or PBS; (D) GPC chromatograms of p(CL_{18}-$DTC_{7.5}$)-PEG micelles with refractive index (RI) detection; spontaneously crosslinked micelles (pink line) were incubated with TCEP (blue line), DTT (green line), or GSH (red line) at a final concentration of 10 mM, for 7 h at 37 °C, and then freeze-dried. The p(CL_{18}-$DTC_{7.5}$)-PEG polymer directly dissolved in DMF was used as a control (black line).

metallic ($Sn(Oct)_2$), have a pronounced influence on the monomer sequence of the resulting copolymers as a consequence of the different polymerization rates of CL and DTC monomers and occurrence of transesterification reactions. Therefore, this study also provides a helpful perspective in selecting the right catalyst, which should have a suitable balance between reactivity and well-controlled polymerization behavior. In addition, the dithiolane-crosslinked micelles showed reduction-responsive behavior (*e.g.*, dissociation in the presence of 10 mM GSH), verifying their suitability for *in vivo* drug delivery applications.

■ ASSOCIATED CONTENT

Supporting Information

The Supporting Information is available free of charge at https://pubs.acs.org/doi/10.1021/acs.macromol.0c01031.

Reaction schemes and molecular structures; monomer conversion kinetics; ^1H and ^{13}C NMR spectra; melting enthalpies and glass-transition temperatures of polymers; sulfhydryl contents by Ellman's assay; GPC chromatograms; dithiolane conversions by UV/vis spectroscopy; and DLS data (PDF)

■ AUTHOR INFORMATION

Corresponding Author

Cornelus F. van Nostrum − *Department of Pharmaceutics, Utrecht Institute for Pharmaceutical Sciences, Utrecht University, 3508 TB Utrecht, The Netherlands;* orcid.org/0000-0003-4210-5241; Phone: +31-620274607; Email: C.F.vannostrum@uu.nl

Authors

Yanna Liu − *Department of Pharmaceutics, Utrecht Institute for Pharmaceutical Sciences, Utrecht University, 3508 TB Utrecht, The Netherlands*

Mies J. van Steenbergen − *Department of Pharmaceutics, Utrecht Institute for Pharmaceutical Sciences, Utrecht University, 3508 TB Utrecht, The Netherlands*

Zhiyuan Zhong − *Biomedical Polymers Laboratory, College of Chemistry, Chemical Engineering and Materials Science, and State Key Laboratory of Radiation Medicine and Protection, Soochow University, Suzhou 215123, P. R. China;* orcid.org/0000-0003-4175-4741

Sabrina Oliveira − *Department of Pharmaceutics, Utrecht Institute for Pharmaceutical Sciences and Division of Cell Biology, Neurobiology and Biophysics, Department of Biology, Utrecht University, 3508 TB Utrecht, The Netherlands;* orcid.org/0000-0002-6011-2122

Wim E. Hennink − *Department of Pharmaceutics, Utrecht Institute for Pharmaceutical Sciences, Utrecht University, 3508 TB Utrecht, The Netherlands;* orcid.org/0000-0002-5750-714X

Complete contact information is available at: https://pubs.acs.org/10.1021/acs.macromol.0c01031

Notes

The authors declare no competing financial interest.

■ REFERENCES

(1) Cameron, D. J. A.; Shaver, M. P. Aliphatic polyester polymer stars: synthesis, properties and applications in biomedicine and nanotechnology. *Chem. Soc. Rev.* **2011**, *40*, 1761–1776.

(2) Seyednejad, H.; Ghassemi, A.; Nostrum, C.; Vermonden, T.; Hennink, W. Functional aliphatic polyesters for biomedical and pharmaceutical applications. *J. Controlled Release* **2011**, *152*, 168−176.
(3) Gaucher, G.; Marchessault, R. H.; Leroux, J.-C. Polyester-based micelles and nanoparticles for the parenteral delivery of taxanes. *J. Controlled Release* **2010**, *143*, 2−12.
(4) BaoLin, G.; Ma, P. X. Synthetic biodegradable functional polymers for tissue engineering: a brief review. *Sci. China: Chem.* **2014**, *57*, 490−500.
(5) Vasir, J. K.; Labhasetwar, V. Biodegradable nanoparticles for cytosolic delivery of therapeutics. *Adv. Drug Delivery Rev.* **2007**, *59*, 718−728.
(6) Kamber, N. E.; Jeong, W.; Waymouth, R. M.; Pratt, R. C.; Lohmeijer, B. G. G.; Hedrick, J. L. Organocatalytic ring-opening polymerization. *Chem. Rev.* **2007**, *107*, 5813−5840.
(7) Albertsson, A.-C.; Varma, I. K. Recent developments in ring opening polymerization of lactones for biomedical applications. *Biomacromolecules* **2003**, *4*, 1466−1486.
(8) Dove, A. P. Organic catalysis for ring-opening polymerization. *ACS Macro Lett.* **2012**, *1*, 1409−1412.
(9) Couffin, A.; Delcroix, D.; Martín-Vaca, B.; Bourissou, D.; Navarro, C. Mild and efficient preparation of block and gradient copolymers by methanesulfonic acid catalyzed ring-opening polymerization of caprolactone and trimethylene carbonate. *Macromolecules* **2013**, *46*, 4354−4360.
(10) Zaremski, M. Y.; Kalugin, D. I.; Golubev, V. B. Gradient copolymers: Synthesis, structure, and properties. *Polym. Sci., Ser. A* **2009**, *51*, 103−122.
(11) Coulembier, O.; Lemaur, V.; Josse, T.; Minoia, A.; Cornil, J.; Dubois, P. Synthesis of poly(l-lactide) and gradient copolymers from al-lactide/trimethylene carbonate eutectic melt. *Chem. Sci.* **2012**, *3*, 723−726.
(12) Pêgo, A. P.; Zhong, Z.; Dijkstra, P. J.; Grijpma, D. W.; Feijen, J. Influence of catalyst and polymerization conditions on the properties of 1,3-trimethylene carbonate and ε-caprolactone copolymers. *Macromol. Chem. Phys.* **2003**, *204*, 747−754.
(13) Wei, J.; Meng, H.; Guo, B.; Zhong, Z.; Meng, F. Organocatalytic ring-opening copolymerization of trimethylene carbonate and dithiolane trimethylene carbonate: impact of organocatalysts on copolymerization kinetics and copolymer microstructures. *Biomacromolecules* **2018**, *19*, 2294−2301.
(14) Fang, J.; Nakamura, H.; Maeda, H. The EPR effect: Unique features of tumor blood vessels for drug delivery, factors involved, and limitations and augmentation of the effect. *Adv. Drug Delivery Rev.* **2011**, *63*, 136−151.
(15) Danhier, F.; Feron, O.; Preat, V. To exploit the tumor microenvironment: Passive and active tumor targeting of nanocarriers for anti-cancer drug delivery. *J. Controlled Release* **2010**, *148*, 135−146.
(16) Deng, C.; Jiang, Y.; Cheng, R.; Meng, F.; Zhong, Z. Biodegradable polymeric micelles for targeted and controlled anticancer drug delivery: Promises, progress and prospects. *Nano Today* **2012**, *7*, 467−480.
(17) Jain, R. K.; Stylianopoulos, T. Delivering nanomedicine to solid tumors. *Nat. Rev. Clin. Oncol.* **2010**, *7*, 653−664.
(18) Tan, C.; Wang, Y.; Fan, W. Exploring polymeric micelles for improved delivery of anticancer agents: recent developments in preclinical studies. *Pharmaceutics* **2013**, *5*, 201−219.
(19) Chauhan, V. P.; Jain, R. K. Strategies for advancing cancer nanomedicine. *Nat. Mater.* **2013**, *12*, 958−962.
(20) Wicki, A.; Witzigmann, D.; Balasubramanian, V.; Huwyler, J. Nanomedicine in cancer therapy: challenges, opportunities, and clinical applications. *J. Controlled Release* **2015**, *200*, 138−157.
(21) Peer, D.; Karp, J. M.; Hong, S.; Farokhzad, O. C.; Margalit, R.; Langer, R. Nanocarriers as an emerging platform for cancer therapy. *Nat. Nanotechnol.* **2007**, *2*, 751−760.
(22) Bae, Y. H.; Yin, H. Stability issues of polymeric micelles. *J. Controlled Release* **2008**, *131*, 2−4.
(23) Ron, N.; Cordia, J.; Yang, A.; Ci, S.; Nguyen, P.; Hughs, M.; Desai, N. Comparison of physicochemical characteristics and stability of three novel formulations of paclitaxel: Abraxane, Nanoxel, and Genexol PM. *Cancer Res.* **2008**, *68*, 5622.
(24) Meng, F.; Hennink, W. E.; Zhong, Z. Reduction-sensitive polymers and bioconjugates for biomedical applications. *Biomaterials* **2009**, *30*, 2180−2198.
(25) Biswas, D.; An, S. Y.; Li, Y.; Wang, X.; Oh, J. K. Intracellular delivery of colloidally stable core-cross-linked triblock copolymer micelles with glutathione-responsive enhanced drug release for cancer therapy. *Mol. Pharmaceutics* **2017**, *14*, 2518−2528.
(26) Brülisauer, L.; Gauthier, M. A.; Leroux, J.-C. Disulfide-containing parenteral delivery systems and their redox-biological fate. *J. Controlled Release* **2014**, *195*, 147−154.
(27) Sadownik, A.; Stefely, J.; Regen, S. L. Regen. Polymerized liposomes formed under extremely mild conditions. *J. Am. Chem. Soc.* **1986**, *108*, 7789−7791.
(28) Li, Y. L.; Zhu, L.; Liu, Z.; Cheng, R.; Meng, F.; Cui, J. H.; Ji, S. J.; Zhong, Z. Reversibly stabilized multifunctional dextran nanoparticles efficiently deliver doxorubicin into the nuclei of cancer cells. *Angew. Chem., Int. Ed.* **2009**, *48*, 9914−9918.
(29) Zou, Y.; Fang, Y.; Meng, H.; Meng, F.; Deng, C.; Zhang, J.; Zhong, Z. Self-crosslinkable and intracellularly decrosslinkable biodegradable micellar nanoparticles: A robust, simple and multifunctional nanoplatform for high-efficiency targeted cancer chemotherapy. *J. Controlled Release* **2016**, *244*, 326−335.
(30) Yang, W.; Zou, Y.; Meng, F.; Zhang, J.; Cheng, R.; Deng, C.; Zhong, Z. Efficient and targeted suppression of human lung tumor xenografts in mice with methotrexate sodium encapsulated in all-function-in-one chimeric polymersomes. *Adv. Mater.* **2016**, *28*, 8234−8239.
(31) Zhu, Y.; Zhang, J.; Meng, F.; Deng, C.; Cheng, R.; Feijen, J.; Zhong, Z. cRGD/TAT dual-ligand reversibly cross-linked micelles loaded with docetaxel penetrate deeply into tumor tissue and show high antitumor efficacy in vivo. *ACS Appl. Mater. Interfaces* **2017**, *9*, 35651−35663.
(32) Zou, Y.; Meng, F.; Deng, C.; Zhong, Z. Robust, tumor-homing and redox-sensitive polymersomal doxorubicin: A superior alternative to Doxil and Caelyx? *J. Controlled Release* **2016**, *239*, 149−158.
(33) Zou, Y.; Zheng, M.; Yang, W.; Meng, F.; Miyata, K.; Kim, H. J.; Kataoka, K.; Zhong, Z. Virus-mimicking chimaeric polymersomes boost targeted cancer siRNA therapy in vivo. *Adv. Mater.* **2017**, *29*, 1−8.
(34) Yang, W.; Xia, Y.; Fang, Y.; Meng, F.; Zhang, J.; Cheng, R.; Deng, C.; Zhong, Z. Selective cell penetrating peptide-functionalized Polymersomes mediate efficient and targeted delivery of methotrexate disodium to human lung cancer in vivo. *Adv. Healthcare Mater.* **2018**, *7*, No. 1701135.
(35) Zhang, N.; Xia, Y.; Zou, Y.; Yang, W.; Zhang, J.; Zhong, Z.; Meng, F. ATN-161 Peptide Functionalized Reversibly Cross-Linked Polymersomes Mediate Targeted Doxorubicin Delivery into Melanoma-Bearing C57BL/6 Mice. *Mol. Pharmaceutics* **2017**, *14*, 2538−2547.
(36) Fang, Y.; Yang, W.; Cheng, L.; Meng, F.; Zhang, J.; Zhong, Z. EGFR-targeted multifunctional polymersomal doxorubicin induces selective and potent suppression of orthotopic human liver cancer in vivo. *Acta Biomater.* **2017**, *64*, 323−333.
(37) Barcan, G. A.; Zhang, X.; Waymouth, R. M. Structurally dynamic hydrogels derived from 1,2-dithiolanes. *J. Am. Chem. Soc.* **2015**, *137*, 5650−5653.
(38) Sadownik, A.; Stefely, J.; Regen, S. L. Polymerized liposomes formed under extremely mild conditions. *J. Am. Chem. Soc.* **1986**, *108*, 7789−7791.
(39) Bang, E. K.; Gasparini, G.; Molinard, G.; Roux, A.; Sakai, N.; Matile, S. Substrate-initiated synthesis of cell-penetrating poly(disulfide)s. *J. Am. Chem. Soc.* **2013**, *135*, 2088−2091.
(40) Margulis, K.; Zhang, X.; Joubert, L. M.; Bruening, K.; Tassone, C. J.; Zare, R. N.; Waymouth, R. M. Formation of polymeric nanocubes by self-assembly and crystallization of dithiolane-containing triblock copolymers. *Angew. Chem., Int. Ed.* **2017**, *56*, 16357−16362.
(41) Wei, R.; Cheng, L.; Zheng, M.; Cheng, R.; Meng, F.; Deng, C.; Zhong, Z. Reduction-responsive disassemblable core-cross-linked micelles based on poly(ethylene glycol)-b-poly(N-2-hydroxypropyl

https://dx.doi.org/10.1021/acs.macromol.0c01031
Macromolecules 2020, 53, 7009−7024

methacrylamide)-lipoic acid conjugates for triggered intracellular anticancer drug release. *Biomacromolecules* **2012**, *13*, 2429−2438.
(42) Zhang, X.; Waymouth, R. M. 1,2-Dithiolane-derived dynamic, covalent Materials: Cooperative self-assembly and reversible cross-linking. *J. Am. Chem. Soc.* **2017**, *139*, 3822−3833.
(43) Zhong, Y.; Zhang, J.; Cheng, R.; Deng, C.; Meng, F.; Xie, F.; Zhong, Z. Reversibly crosslinked hyaluronic acid nanoparticles for active targeting and intelligent delivery of doxorubicin to drug resistant CD44+ human breast tumor xenografts. *J. Controlled Release* **2015**, *205*, 144−154.
(44) Pratt, R. C.; Nederberg, F.; Waymouth, R. M.; Hedrick, J. L. Tagging alcohols with cyclic carbonate: a versatile equivalent of (meth)acrylate for ring-opening polymerization. *Chem. Commun.* **2008**, 114−116.
(45) Delcroix, D.; Martín-Vaca, B.; Bourissou, D.; Navarro, C. Ring-opening polymerization of trimethylene carbonate catalyzed by methanesulfonic acid: Activated monomer versus active chain end mechanisms. *Macromolecules* **2010**, *43*, 8828−8835.
(46) Lohmeijer, B. G. G.; Pratt, R. C.; Leibfarth, F.; Logan, J. W.; Long, D. A.; Dove, A. P.; Nederberg, F.; Choi, J.; Wade, C.; Waymouth, R. M.; Hedrick, J. L. Guanidine and Amidine Organocatalysts for ring-opening polymerization of cyclic esters. *Macromolecules* **2006**, *39*, 8574−8583.
(47) Bagheri, M.; Bresseleers, J.; Varela-Moreira, A.; Sandre, O.; Meeuwissen, S. A.; Schiffelers, R. M.; Metselaar, J. M.; van Nostrum, C. F.; van Hest, J. C. M.; Hennink, W. E. Effect of formulation and processing parameters on the size of mPEG-*b*-p(HPMA-Bz) polymeric micelles. *Langmuir* **2018**, *34*, 15495−15506.
(48) Delcroix, D.; Couffin, A.; Susperregui, N.; Navarro, C.; Maron, L.; Martin-Vaca, B.; Bourissou, D. Phosphoric and phosphoramidic acids as bifunctional catalysts for the ring-opening polymerization of ε-caprolactone: a combined experimental and theoretical study. *Polym. Chem.* **2011**, *2*, 2249−2256.
(49) Susperregui, N.; Delcroix, D.; Martin-Vaca, B.; Bourissou, D.; Maron, L. Ring-opening polymerization of epsilon-caprolactone catalyzed by sulfonic acids: computational evidence for bifunctional activation. *J. Org. Chem.* **2010**, *75*, 6581−6587.
(50) Bordwell, F. G. Equilibrium acidities in dimethyl sulfoxide solution. *Acc. Chem. Res.* **1988**, *21*, 456−463.
(51) Pratt, R. C.; Lohmeijer, B. G.; Long, D. A.; Waymouth, R. M.; Hedrick, J. L. Triazabicyclodecene: a simple bifunctional organocatalyst for acyl transfer and ring-opening polymerization of cyclic esters. *J. Am. Chem. Soc.* **2006**, *128*, 4556−4557.
(52) Albertsson, A.-C.; Eklund, M. Synthesis of copolymers of 1,3-dioxan-2-one and oxepan-2-one using coordination catalysts. *J. Polym. Sci., Part A: Polym. Chem.* **1994**, *32*, 265−279.
(53) Matyjaszewski, K.; Ziegler, M. J.; Arehart, S. V.; Greszta, D.; Pakula, T. Gradient copolymers by atom transfer radical copolymerization. *J. Phys. Org. Chem.* **2000**, *13*, 775−786.
(54) Kamber, N. E.; Jeong, W.; Waymouth, R. M.; et al. Organocatalytic ring-opening polymerization. *Chem. Rev.* **2007**, *107*, 5813−5840.
(55) Odian, G. *Principles of Polymerization*; Wiley-Interscience:Hoboken, NJ, 2004; pp 545−568.
(56) Schindler, A.; Hibionada, Y. M.; Pitt, C. G. Aliphatic polyesters. III. molecular weight and molecular weight distribution in alcohol-Initiated polymerizations of ε-caprolactone. *J. Polym. Sci., Polym. Chem. Ed.* **1982**, *20*, 319−327.
(57) Loontjens, C. A. M.; Vermonden, T.; Leemhuis, M.; van Steenbergen, M. J.; van Nostrum, C. F.; Hennink, W. E. Synthesis and characterization of random and triblock copolymers of ε-caprolactone and (Benzylated)hydroxymethyl glycolide. *Macromolecules* **2007**, *40*, 7208−7216.
(58) Clément, B.; Grignard, B.; Koole, L.; Jérôme, C.; Lecomte, P. Metal-free strategies for the synthesis of functional and well-defined polyphosphoesters. *Macromolecules* **2012**, *45*, 4476−4486.
(59) Ling, J.; Zhu, W.; Shen, Z. Controlling ring-opening copolymerization of ε-caprolactone with trimethylene carbonate by scandium tris(2,6-di-tert-butyl-4-methylphenolate). *Macromolecules* **2004**, *37*, 758−763.
(60) Yang, L.-Q.; Yang, D.; Guan, Y.-M.; Li, J.-X.; Li, M. Random copolymers based on trimethylene carbonate and ε-caprolactone for implant applications: Synthesis and properties. *J. Appl. Polym. Sci.* **2012**, *124*, 3714−3720.
(61) Pastusiak, M.; Dobrzynski, P.; Kasperczyk, J.; Smola, A.; Janeczek, H. Synthesis of biodegradable high molecular weight polycarbonates from 1,3-trimethylene carbonate and 2,2-dimethyltrimethylene carbonate. *J. Appl. Polym. Sci.* **2014**, *131*, No. 40037.
(62) Wennink, J. W. H.; Liu, Y.; Makinen, P. I.; Setaro, F.; de la Escosura, A.; Bourajjaj, M.; Lappalainen, J. P.; Holappa, L. P.; van den Dikkenberg, J. B.; Al Fartousi, M.; Trohopoulos, P. N.; Yla-Herttuala, S.; Torres, T.; Hennink, W. E.; van Nostrum, C. F. Macrophage selective photodynamic therapy by meta-tetra(hydroxyphenyl)chlorin loaded polymeric micelles: A possible treatment for cardiovascular diseases. *Eur. J. Pharm. Sci.* **2017**, *107*, 112−125.
(63) Carstens, M. G.; Bevernage, J. J. L.; van Nostrum, C. F.; van Steenbergen, M. J.; Flesch, F. M.; Verrijk, R.; de Leede, L. G. J.; Crommelin, D. J. A.; Hennink, W. E. Small oligomeric micelles based on end group modified mPEG−oligocaprolactone with monodisperse hydrophobic blocks. *Macromolecules* **2007**, *40*, 116−122.
(64) Iyer, K. S.; Klee, W. A. Direct spectrophotometric measurement of the rate of reduction of disulfide bonds. The reactivity of the disulfide bonds of bovine -lactalbumin. *J. Biol. Chem.* **1973**, *248*, 707−710.
(65) Han, J. C.; Han, G. Y. A procedure for quantitative determination of Tris(2-carboxyethyl)phosphine, an odorless reducing agent more stable and effective than dithiothreitol. *Anal. Biochem.* **1994**, *220*, 5−10.
(66) Meng, H.; Zou, Y.; Zhong, P.; Meng, F.; Zhang, J.; Cheng, R.; Zhong, Z. A smart nano-prodrug platform with reactive drug loading, superb stability, and fast responsive drug release for targeted cancer therapy. *Macromol. Biosci.* **2017**, *17*, No. 1600518.
(67) Gasparini, G.; Sargsyan, G.; Bang, E. K.; Sakai, N.; Matile, S. Ring tension applied to thiol-mediated cellular uptake. *Angew. Chem., Int. Ed.* **2015**, *54*, 7328−7331.
(68) Carmine, A.; Domoto, Y.; Sakai, N.; Matile, S. Comparison of lipoic and asparagusic acid for surface-initiated disulfide-exchange polymerization. *Chemistry* **2013**, *19*, 11558−11563.
(69) Burns, J. A.; Whitesides, G. M. Predicting the stability of cyclic disulfides by molecular modeling: "effective concentrationsin" thiol-disulfide interchange and the design of strongly reducing dithiols. *J. Am. Chem. Soc.* **1990**, *112*, 6296−6303.

https://dx.doi.org/10.1021/acs.macromol.0c01031
Macromolecules 2020, 53, 7009−7024